GLOW DISCHARGE ENHANCED CHEMICAL REACTION: APPLICATION IN AMMONIA SYNTHESIS AND HYDROCARBON GAS CLEANUP

A Thesis

by

PINGJIA MING

Submitted to the Office of Graduate Studies and Professional Studies of
Texas A&M University
In partial fulfillment of the requirement for the degree of

MASTER OF SCIENCE

Chair of Committee,	David Staack
Committee Members,	Kalyan Annamalai
	Mehrdad Ehsani
Head of Department,	Andreas Polycarpou

August 2014

Major Subject: Mechanical Engineering

ABSTRACT

Two different plasma enhanced processing technologies were investigated in this study: ammonia synthesis from steam and nitrogen, and hydrocarbon gas clean up.

Ammonia is a common sanitizer in swimming pool and fish tank, changing the pH of the water, which does not benefit bacteria. Also ammonia is used in various NO_x reduction technologies, for example, selective catalytic reduction (SCR) methods have been studied for the cleaning of diesel engine exhaust. A small compact glow discharge was applied to investigate ammonia synthesis from steam and nitrogen. Ammonia was successfully detected via UV-VIS absorbance and through increasing pH value of treated water by product gas.

Heavier hydrocarbon C_3 to C_5 are produced with natural gas, but cannot be used in sensitive energy conversion systems, like solid oxide fuel cell (SOFC). Utilizing small amount of energy to clean up and reform heavier hydrocarbon into synthesis gas is necessary when using hydrocarbon sources which contain heavier hydrocarbons mixture such as EPE (74.8% methane, 8% ethane, 8% ethylene, 2.1% propane and 1.1% Propene). Non-thermal plasmas, due to their unique non-equilibrium characteristics, offer advantages as method of reforming at lower temperature (100-150 ^oC) and atmospheric pressure. For an EPE gas mixture, a high conversion and low specific energy cost is desirable. Variation in discharge power density, air and, water addition were tested, in order to find conditions which were energetically feasibility, efficiency

and sufficiently reduced the higher hydrocarbon. High conversion efficiency was achieved, in propane and propene, which was more than 90%, without carbon deposition through air addition. For a 1 J/ml power density and 1.08 O_2/C ratio condition, a process efficiency of 74% and 54% available output energy was achieved. At the same time, the concentration of ethane, ethylene, propane, propylene, and acetylene were cleaned-up to value of 1.01%, 1.67%, 0.08%, 0.00%, and 0.50%, respectively, less than 20% of their original input amount. Higher power density produced cleaner (less high hydrocarbons) in the products, and were still energetically feasible, but less efficient.

DEDICATION

To my parents who support me, Zhang Hong, Ming Daojun.

ACKNOWLEDGEMENTS

I would like to express my sincere gratitude to Dr. David Staack for all the guidance and support he has provided me in the past couple of years.

I would like to thank my committee members, Dr. Kalyan Annamalai and Dr. Ehsani Mehrdad, for their valuable input.

I would like to thank Robert Geiger and PEDL mates for sharing their knowledge and helping me in my experimental work

NOMENCLATURE

DBD	Dielectric Barrie Discharge
POX	Partial Oxidation
SR	Steam Reforming
DR	Dry Reforming
GC	Chromatography
MS	Mass Spectrometer
LHVP	Low Heating Value Power
H_2O/C	H_2O/C is Mole Ratio, C Only Counts from Hydrocarbons
O_2/C	O_2/C is Mole Ratio, C Only Counts from Hydrocarbons

TABLE OF CONTENTS

Pages

LIST OF FIGURES

Page

LIST OF TABLES

Page

1. INTRODUCTION

Application of plasma technologies today are numerous and involve many industries. High-energy efficiency, high specific productivity, and high selectivity may be achieved in plasma for wide range of chemical processes. Inorganic gas-phase plasma decomposition processes, for example, carbon dioxide dissociation, triatomic molecules dissociation: NH_3, SO_2, and N_2O. Also Gas phase inorganic synthesis nitrogen oxides from air and ozone generation and Plasma-chemical fuel conversion and hydrogen production.[1] Ammonia synthesis from steam and nitrogen, and hydrocarbon gas cleanup will be discussed in this work.

1.1 Ammonia synthesis

Ammonia is a common ingredient in sanitizer.[2] A method of sanitizing a volume of water, such as a swimming pool and fish tank, is changing the pH of the water, which does not benefit bacteria. Two methods are common, one being used when the pH of the water in conjunction with chlorine, and a bromine-containing material which keep water pH at slight acid. Another method provides addition of species like ammonia which keep water pH at basic region.[3] Ammonia is also used in various NO_x reduction technologies, such as the selective catalytic reduction (SCR) methods have been studied for the cleaning of diesel engine exhaust. The SCR system, in which ammonia is used as a reducing agent, is thought to be one of the most promising methods for emissions control.[4] In both sanitation and emissions applications the

development of compact, point of use methods of ammonia synthesis, such as the plasma system investigated in the thesis, are desirable.

None-equilibrium glow discharge plasma reforming which eliminates the need for catalyst operated at lower temperature, atmosphere pressure and low power requirement. For non-thermal plasma, already proved have a promising success in fuel reforming, which character with higher efficiency, especially gliding arc plasma.[1] A type of gliding arc plasma was chosen to synthesis ammonia in this investigation.

The overall chemical reaction pathway in the reforming process is $N_2 + 3H_2O \rightarrow 2NH_3 + 1.5O_2$, with the initial water and nitrogen dissociation facilitated by high energy electron in the plasma.

1.2 Hydrocarbon gases cleanup

Natural gas is a vital component of the world's supply of energy. It is one of the cleanest, safest, and most useful of all energy sources.[5] there are 2,543 trillion cubic feet of technically recoverable natural gas in the United States. This includes undiscovered, unproved, and unconventional natural gas.[6] Natural gas is a combustible mixture of hydrocarbon gases. While natural gas is formed primarily of methane, it can also include ethane, propane, butane and pentane. The composition of natural gas can vary widely, but Table 1 below outlines the typical makeup of natural gas before it is refined.

Table 1. Typical composition of natural gas[6]

Methane	CH_4	70-90%
Ethane	C_2H_6	0-20%
Propane	C_3H_8	
Butane	C_4H_{10}	
Carbon Dioxide	CO_2	0-8%
Oxygen	O_2	0-0.2%
Nitrogen	N_2	0-5%
Hydrogen Sulfide	H_2S	0-5%
Rare Gases	Ar, He, Ne, Xe	trace

Natural gas was used in variety of area. The domestic use is a powerful heating and cooking fuel. Natural gas is a major source of electricity generation through the use of cogeneration, gas turbines and steam turbines. Natural gas is a main feedstock of ammonia synthesis, used for fertilizer production. Natural gas is main source of hydrogen production. And several synthesis gas production methods are available, depending on the purpose of industrial application i.e., steaming reforming, dry reforming and partial oxidation. Natural gas is also used in the manufacture of fabrics, glass, steel, plastics, paint etc. Summary main route of the main content of natural gas, methane, have been investigated utilization in figure 1. [7]

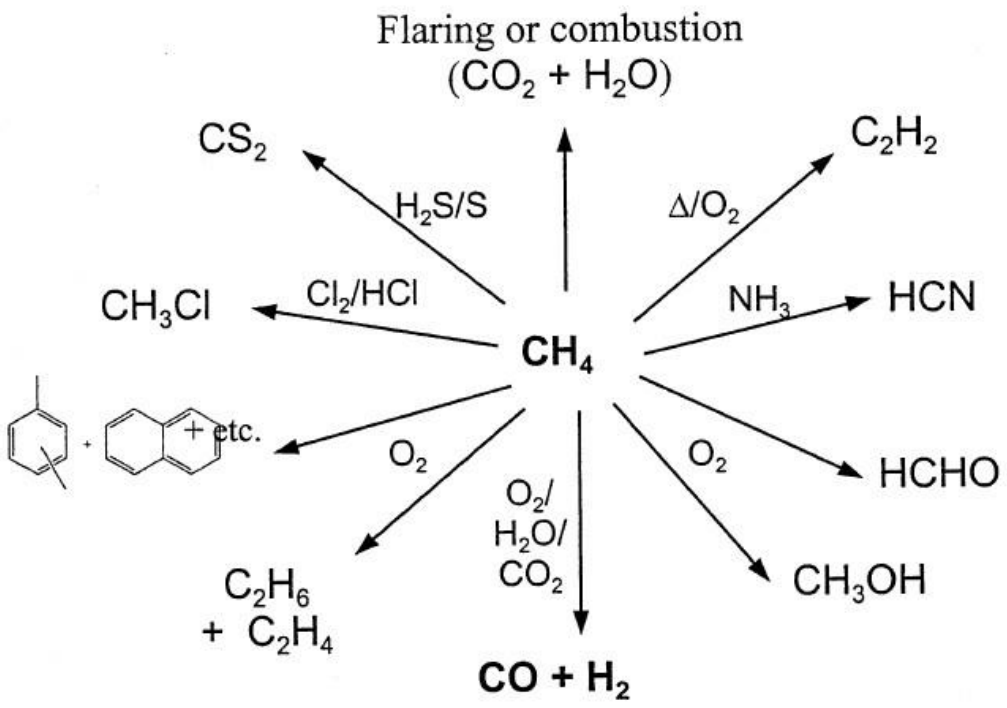

Figure 1. Summary of methane conversion routes [7]

Synthesis gas, as fuel for power generation by fuel cell, draws more and more attention. Unlike traditional combustor, internal combustion engines and gas turbine, fuel cell works more silently, less noisy, and potentially more efficiently. Compared with air fuel combustion process, the emissions are cleaner with no particulate matter (mostly soot) and few toxic substances in the fuel cell exhaust.

Increasing pollution of air-fuel combustion process from vehicles and power plants is leading to development of alternate energy generation techniques like fuel cells. Since the products are mainly water and less undesirable noxious, which have lower

impact on environment. Moreover, high temperature fuel cell system is better tolerance of fuel gas than lower temperature fuel cell system. Melt carbonate fuel cells and solid oxide fuel cell system both can run with hydrogen, carbon monoxide, methane and tolerate carbon dioxide.[8] A hydrocarbon reforming process through is essential for preprocessing the feed-in fuel gas which may contain components incompatible with fuel cell process and material. Fuel cell also has a huge potential as a power source on vehicle and in small scale applications. The challenge with on-board, and point of use fuel processing is to transfer large-scale industrial processes, such as steam reforming or partial oxidation, to lightweight and compact reactors that fit in small footprints like a standard-size vehicle. The power density and non-thermal mechanism of plasma reformers offer the possibility of a lower temperature smaller system.

The processing of hydrocarbons to hydrogen-rich reformate is usually done by steam reforming, partial oxidation, or a combination of both.[8] Details on these processes are given in chapter 2 as background. Important to remember is that breaking up a large hydrocarbon typically requires a significant amount of activation energy. The plasma can provide this energy directly, though not always efficiently. Oxidizing part of the fuel with air or O_2 (called partial oxidation) can also provide some of the energy but consumes fuel. Using water as a source of oxygen (called the water–shift) with less free energy is also possible and has benefits of producing hydrogen.

The kinetic rates of the reactions which need to take place are also important and are highly temperature dependent. The kinetic limitations of fuel conversion processes

often require higher reaction temperatures than what is necessary to produce the same results when the system is at thermodynamic equilibrium. Lower reaction temperatures are desired not only from the obvious viewpoint of improving energy efficiency, but because higher temperatures can open reaction pathways that may ultimately lead to undesirable coking and soot formation in hydrocarbon reforming systems. Therefore, many modern fuel conversion systems incorporate a catalyst of some kind in order to lower activation energy barriers and thus lower the required reaction temperatures and avoid unwanted by-product formation.[9]

Many of hydrocarbon conversion systems are operated with assistance from metal catalysts, such as nickel, platinum, and rhodium, in order to accelerate the fuel conversion reactions and lower the required reaction temperatures.[9] The catalyst process are expensive, due to the rare metals and also it need process at a high temperature to keep catalyst active.

Plasma works as an alternative to traditional catalysts in fuel reforming. Researchers that incorporate plasma into fuel reforming systems claim that plasma behaves like a catalyst without temperature limit.[1] The effect of plasma catalysis, in essence, is caused by the interaction of charged and excited particles generated by plasma that allows for the reduction or removal of activation energy barriers in fuel conversion reactions.[9] Examples of several plasma initiated chemical reactions are given below. These reactions are typically require very high temperatures to be thermally activated at significant rates. Plasmas have a possible advantage over thermal

processes in that only the electrons (not all of the gas components) need to be high temperature.

$$e^- + N_2 \rightarrow \dot{N} + \dot{N} + e^- \quad (1)$$

$$e^- + H_2O \rightarrow \dot{HO} + \dot{H} + e^- \quad (2)$$

$$e^- + CH_4 \rightarrow C\dot{H}_3 + \dot{H} + e^- \quad (3)$$

$$e^- + C_2H_6 \rightarrow C_2\dot{H}_5 + \dot{H} + e^- \quad (4)$$

$$e^- + C_3H_8 \rightarrow C_3\dot{H}_7 + \dot{H} + e^- \quad (5)$$

For the research presented in this thesis, a non-thermal plasma was applied. Non-thermal plasma also called non-equilibrium plasma as covered in detail in the background sections of chapter 2. In non-equilibrium plasma, the electron temperature is equal or greater than 10000 K, and the vibrational temperature ranges 1000K to several thousand K, however, the gas temperature can be room temperature to several hundred ºC. Because of this characteristic, non-thermal plasma can process low temperature chemical process. In this process, rector temperature was control in the range of 100 ºC to 150 ºC. Compared with thermal process, plasma process can operate at low temperature and also low pressure. For comparison, in order to get hydrogen and monoxide in products through an equilibrium process, the temperature must be operated above 1000 ºC in thermal process, as shown in figure 2.

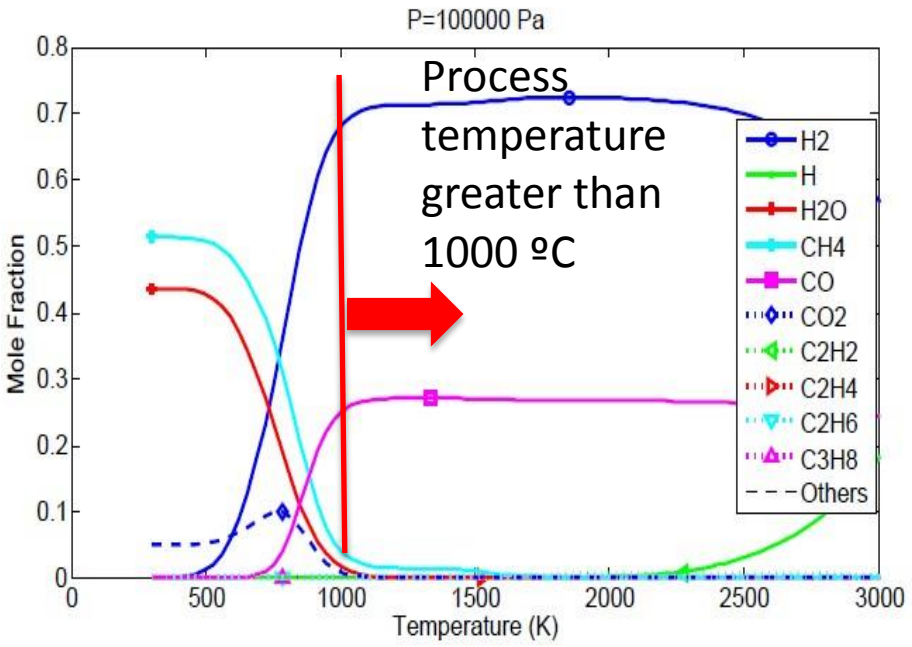

Figure 2. Thermal equilibrium analysis via Cantera and gri30 mechanism simulation at H2O/C ratio=1

1.3 Thesis objectives and summary

Several tasks and goals are seen as necessary to complete as part of this investigation of glow discharges as chemical reactors and are briefly described below and addressed in the contents of this thesis.

First was to design and experimentally build a glow discharge reactor system with power control, applied magnetic field to confine the glow discharge, and temperature control system, which enable reactor work at range of room temperature to 200ºC. Flow control systems, and system for generation of steam and water for

introduction of reactant into the reactor were also needed. The final design of this system and procedures for its use are addressed in Chapter 3 of this thesis.

Second was the application of the system to investigate ammonia synthesis from nitrogen and steam at relatively low temperature. A variety of methods were used to diagnose ammonia in products, including UV-VIS absorbance study, and several types of pH value measurement These were used to identify ammonia in the product and determine the rates of production. The results of ammonia synthesis are presented in the first section of Chapter 5 and the diagnostics methods are presented in chapter 4.

The majority of work focuses on the two different reforming methods (steam reforming and auto-thermal process) will be studied to clean up heavier hydrocarbon. Diagnostics were developed for measuring the various hydrocarbon concentrations using GC and MS as well as the plasma parameters, these are described in chapter 4. A first set of experiments investigated trends in the conversion rate of heavier hydrocarbons, under air and steam addition, and different power density input. This also studied different H_2O/C ratio, O_2/C ratio, and power density influence on cleanup results. An important consideration was on the H_2/CO ratio study and minimizing carbon formation. From the initial studies trend for optimization were noted including power density, O_2/C and H_2O ratio which benefit cleanup result and high efficiency. Process efficiency was calculated from experimental parameters and product gas concentrations. Feasibility of the process was determined from the ratio between plasma power and potential electricity power generated from cleaned-up products. The level of clean-up was also quantified, with

parameters chosen so that product concentration of each C_2 & C_3 will be less than 20% of their original concentration (this corresponds to what is referred to as less than 20% slip). All of these hydrocarbon processing results are presented in Chapter 5.

A summary of this work and discussions about future work are presented in the final chapter, Chapter 6. Generally a working discharge system was built and diagnosed. Proof of concept ammonia generation was demonstrated in a small scale reactor. For hydrocarbon clean-up results shown efficient and feasible processing but will require further development before it could be commercially viable.

2. THE APPLICATION OF PLASMA AND LITERATURE REVIEW

2.1 The common reforming processes

2.1.1 Pyrolysis

Pyrolysis is known as decomposition of hydrocarbons at high temperature or plasma without any other oxidizer like oxygen, water, and carbon dioxide. Pyrolysis is an endothermic process and produce hydrogen and solid carbon C_2 at sufficient high temperature.

$C_nH_m \rightarrow nC\ (s) + m2H_2$

Refer to methane pyrolysis

$CH_4 \rightarrow 2H_2 + C\ (s),\ \Delta H = 74.81\ kJ\ mol^{-1}$

2.1.2 Partial oxidation

The partial oxidation (POX) of hydrocarbon fuel is hydrocarbons burning in an oxygen lean condition. The stoichiometric reaction [O]/[C] ratio equal to 1. This reaction is mildly exothermic; it will start its own without any heating process. The gliding arc discharges are well suited for this due to their ability to remain strongly non-equilibrium and mostly non-thermal even at relatively high power levels.[1]

$C_nH_m + n2O_2 \rightarrow nCO + m/2H_2$

Often referred to specific partial oxidation are:

$CH_4 + 1/2O_2 \rightarrow 2\ H_2 + CO,\ \Delta H = -\ 43.6\ kJ\ mol^{-1}$

$C_2H_4 + O_2 \rightarrow 4\ H_2 + 2CO,\ \Delta H = -\ 273.5\ kJ\ mol^{-1}$

$C_2H_6 + O_2 \rightarrow 2\ H_2 + 2CO,\ \Delta H = -\ 136.4\ kJ\ mol^{-1}$

$C_3H_6 + 3/2\ O_2 \rightarrow 3\ H_2 + 3\ CO,\ \Delta H = -\ 352.0\ kJ\ mol^{-1}$

$C_3H_8 + 3/2\ O_2 \rightarrow 4\ H_2 + 3\ CO,\ \Delta H = -\ 227.74\ kJ\ mol^{-1}$

The hydrogen yield in POX is usually limited by the formation of water

2.1.3 Dry reforming

Carbon dioxide as oxidizer reacts with hydrocarbons and produce synthesis gas.

$C_nH_m + nCO_2 \rightarrow 2nCO + m2H_2$

$CH_4 + CO_2 \rightarrow 2H_2 + 2\ CO,\ \Delta H = 247.9\ kJ\ mol^{-1}$

Carbon dioxide as greenhouse gas is mainly produced form fossil fuel combustion. Removing CO_2 from exhaust flow of power plants is a new idea recently. Plasma recovery of CO_2 has been investigated as environment control.[10] Higher percentage of CO_2 in natural gas field is often encountered. Dry reforming provides a directly method to utilize in these natural gas field.

2.1.4 Steam reforming

The water vapor oxides the hydrocarbons process generate syngas. The reaction is endothermic process and its need to preheat up to initiate. However, due to water gas shift reaction, steam reforming generates hydrogen-rich products.

$C_nH_m + nH_2O \rightarrow nCO + (m/2 + n)H_2$

Reaction enthalpy of steam reforming:

$CH_4 + H_2O \rightarrow 3\ H_2 + CO,\ \Delta H = 206.2\ kJ\ mol^{-1}$

$C_2H_4 + 2H_2O \rightarrow 4\ H_2 + CO,\ \Delta H = 210.1\ kJ\ mol^{-1}$

$C_2H_6 + 2H_2O \rightarrow 5\ H_2 + 2CO,\ \Delta H = 347.3\ kJ\ mol^{-1}$

$C_3H_6 + 3H_2O \rightarrow 6\ H_2 + 3\ CO,\ \Delta H = 373.5\ kJ\ mol^{-1}$

$C_3H_8 + 3H_2O \rightarrow 8\ H_2 + 3\ CO,\ \Delta H = 497.7\ kJ\ mol^{-1}$

The two processes SR and POX may be combined by supplying both steam and air to the reformer and adjusting the ratio of oxygen and steam to tune the thermal balance of the reactor. In principle, the reaction enthalpy can be set to zero; this is why the process is called auto-thermal reforming. In fact, a direct temperature regulation of the reactor by the reactant ratio is conceivable. In addition to thermal management, auto-thermal reforming also offers control of the molar product ratio, which makes it attractive as a source of syngas.[11]

2.1.5 Water gas shift reaction

Water shift reaction, in practical, increases hydrogen in products. Due to water shift reaction, below, is slightly exothermic reaction.

$CO + H_2O(g) \rightarrow CO_2 + H_2,\ \Delta H = -41.1\ kJ\ mol^{-1}$

In raw reforming products, mainly consists of hydrogen, and carbon monoxide, carbon dioxide and unreformed fuel. Presence of steam will convert carbon monoxide into carbon dioxide and more hydrogen in products at lightly higher temperature.

However, the kinetic limitations of fuel conversion processes often require higher reaction temperatures than what is necessary to produce the same results when the system is at thermodynamic equilibrium. Lower reaction temperatures are desired not only from the obvious viewpoint of improving energy efficiency, but because higher

temperatures can open reaction pathways that may ultimately lead to undesirable coking and soot formation in hydrocarbon reforming systems. Therefore, many modern fuel conversion systems incorporate a catalyst of some kind in order to lower activation energy barriers and thus lower the required reaction temperatures and avoid unwanted by-product formation.[9]

2.2 Plasma physics

Plasma is described as the fourth state of matter. Unlike solid, liquid and gas, plasma usually character with high energy, chemical reactive and thermal such as lightning. It consists of positive and negative ions, electrons, radicals, and neutral gas atoms and molecules.[12] Plasmas are generally classified as thermal or non-thermal plasma. Thermal plasma can at gas temperatures on the order of 10,000 K or even higher. A thermal plasma is considered to be at equilibrium state and follows the major laws of thermodynamics can be characterized by a single temperature at each point space because the mean electrons temperature, which is high temperature in plasma, is equal to the gas temperature, $T_e = T_{gas}$.[1] Non-thermal plasma is conventionally in weakly ionization plasma, the temperature could be $T_e > T_v > T_r \approx T_i \approx T_0$. Non-thermal plasma temperature can be as low as room temperature. Due to non-thermal nature, non-thermal plasma can remain chemical active without excessive heat. It's widely used in film deposition, synthesis, lighting source etc.

2.2.1 Current-voltage characteristic of discharge between electrodes

Discharges are studied by current-voltage characteristics, and the current density, and breakdown voltage. These main characteristics mainly depend on the discharge gap, pressure inside tube, gas, and electrode material as shown in figure 3.

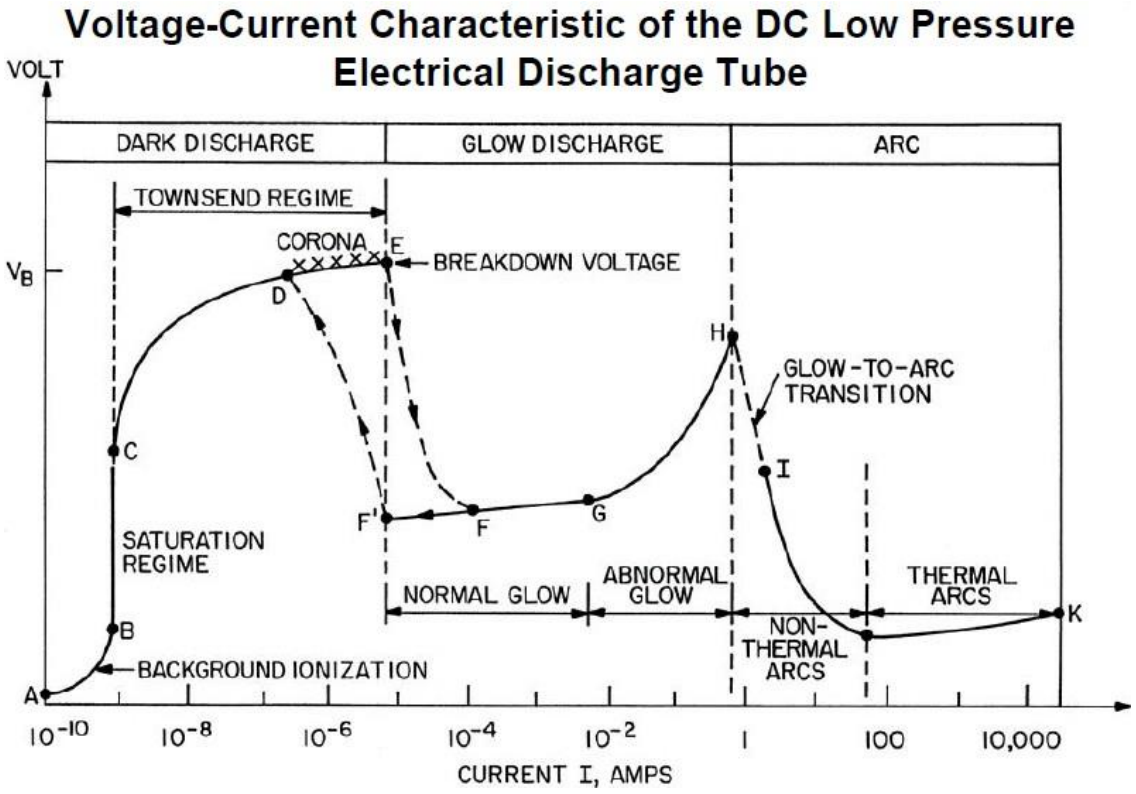

Figure 3. Current-voltage characteristic of discharge between electrodes[13]

2.2.2 Dark discharges

The regions between A to E is dark discharge region, except corona has weak lumination. At background ionization stage, the ions and electrons are originates from cosmic. It produces constant low charge density and low degree ionization at atmospheric pressure. With increasing voltage, more electrons and ions accumulate at electrodes, while the current increases. Current saturation happens at(B-C) while increasing field potential. When voltage high enough, electric field initially "charge" the electrons, whose energy is sufficient to ionize the neutral particles. The avalanche process has started from secondary electrons emission generating new electrons. Avalanche process prepares for breakdown, yet the breakdown not happen at Townsend discharge (C-E).

2.2.3 Corona discharge

Corona happens at such as sharp corners, projecting points, edges of metal surfaces, or small diameter wires at high potential regions. Not the whole corona discharge can be visible, while the current is high enough to visible by eyes. The visible corona is part of the discharge; it doesn't occupy space between electrodes. Moreover, the corona discharge belongs to dark discharge (D-E).

2.2.4 Electrical breakdown

The electrical breakdown occurs in Townsend regime when the ions reaching the cathode have sufficient energy to generate secondary electrons(E). Photon impact is a different possible process for generating secondary electrons. At the breakdown, or

sparking potential V_B, the current might increase by a factor of 10^4 to 10^8. Only the internal resistance of the power supply connecting the two electrodes usually limits it. If the current supply is to low, discharge tube cannot draw enough current to break down the gas, and the tube will remain in the corona regime with small corona points or brush discharges being visible at the electrodes. If power supply delivers enough current, the gas will break down at the voltage V_B, and avalanche processes will occurred and the discharge will move into the normal glow discharge regime. The breakdown voltage for a particular gas and electrode material depends on the product of the pressure and the distance between the electrodes, as expressed in Paschen's law.

2.2.5 Glow discharge

The glow discharge regime owes its name to the typical luminous glow. The plasma gas emits light because the electron energy and number density are high enough to generate excited gas atoms by collisions. These excited gas atoms will eventually relax to their ground state by emission of photons. The applications of glow discharge include fluorescent lights (Neon tubes), dc parallel plate plasma reactors, used for depositing thin films. Glow discharges are also extensively used in plasma chemistry.

After a discontinuous transition from E to F, the gas enters the normal glow region (F - G), in which the voltage is almost independent of the current over several orders of magnitude in the discharge current. This current-voltage behavior is very different from a normal Ohm type resistance. The electrode current density does not change with the total current in this regime. Only a small part of the cathode surface at

low currents is in contact with the plasma. As the current increases from F to G, the fraction of the cathode occupied by the plasma increases, until plasma covers the entire cathode surface at point G. The discharge voltage remains constant over a large range of current variation.

Once the whole surface of the cathode is covered by the discharge, the only way the total current can increase further is to drive more current through the cathode by increasing the current density. This requires more energy, applying more voltage moving away from the Paschen minimum. This regime where the voltage increases significantly with the increasing total current (G-H) is named the abnormal glow regime. The discharge now behaves here more like a normal resistance. Starting at point G and decreasing the current, a form of hysteresis is observed in the voltage-current characteristic. The discharge maintains itself at considerably lower currents and current densities than at point F and only then makes a transition back to Townsend regime.

In the abnormal discharge the cathode fall potential increases rapidly, and the dark space shrinks. Except for being brighter, the abnormal glow discharge resembles the normal discharge. The structures near the cathode may blend into one another and a rather uniform glow can be observed. At the same time as voltage and cathode current density increase the average ion energy bombarding the cathode surface also increases. Due to the high current density abnormal discharges are commonly used as sputter sources. The bombardment with ions ultimately heats the cathode causing thermionic

emission. Once the cathode is hot enough to emit electrons thermionically, the discharge will change to an arc regime.

2.2.6 Arc discharges

At point H, the electrodes become sufficiently hot that the cathode emits electrons thermionically. If sufficient current is supplied to the discharge it will undergo a glow-to-arc transition, (H-I). The arc regime, from I through K is one where the discharge voltage decreases as the current increases, until large currents are achieved at point J, and after that the voltage increases again slowly with increasing current.[14]

2.3 Type of discharge

2.3.1 Corona

A corona discharge is a weakly luminous discharge, and in some cases not very visible to the naked eye. Coronas appear at atmospheric pressures near sharp electrodes or points where the electric field is very high. The electron emission mechanism in Coronas is secondary electron emission. Coronas appear in the Dark Discharge Regime.

2.3.2 Glow discharge

The glow discharge is the best –known type of non-thermal discharge and has been widely used in plasma chemistry for more than a century. The term “glow” indicates that the plasma of the discharge is luminous in contrast to the relatively low-power dark discharge.[1] Glow discharge is, unlike microwave discharge, an electrode needed, direct current (DC), and self-sustained discharge. Glow discharge consists of

Aston dark space, Cathode glow, Cathode dark space, Negative glow, Faraday dark space, Positive column, and Anode glow and anode dark space, shown in figure 4.

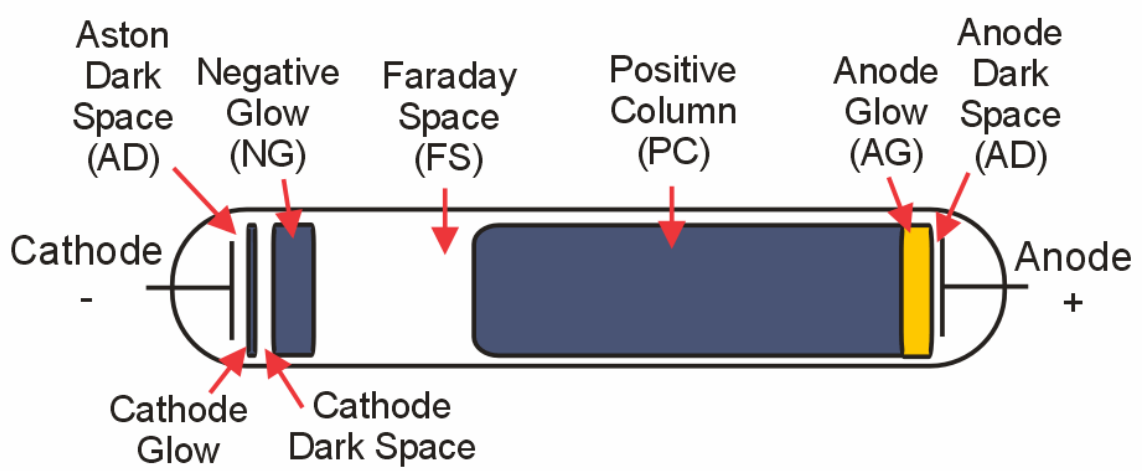

Figure 4. Glow discharge regions [15]

The electric potential between electrode gap doesn't linearly change with distance, a distinctive potential drop near cathode, named potential fall. The potential drop voltage is about 100-500 V depend on material of cathode and property gas in between. Cathode fall voltage in different cathode material and gases shown in table 2 [12]

Table 2. Normal cathode fall voltage (unit:V)

gas Cathode	air	H2	N2	O2	CO	CO2
Al	229	170	180	311	-	-
Cu	370	214	208	-	484	460
Fe	269	250	215	290	-	-

Electron temperature (T_e), vibrational temperature (T_{vib}), rotational temperature (T_{rot}) and translational temperature (T_{trans}) are known as non-equilibrium plasma characteristics, like glow discharge typically $T_e > T_{vib} > T_{rot} = T_{trans}$. An atmospheric pressure DC glow discharge with1550 K rotational temperature and 4500K vibrational temperature via measuring the 2nd positive band of N_2 operated at 10 mA. The voltage-current characteristics indicated that the discharge is operating in the normal glow regime. The glow discharge was generated in between a cylindrical and a flat cathode and the gap varied from 20μm to 1.5 cm.[16] The DC glow discharge's temperature was measure as function of temperature from 50μA to 30mA, and discharge length, ranging from 50μm to 1mm. The Rotational temperature from 400K to 2000K was measured, and vibrational temperature varied from 2000K to as high as 5000K in that work.[17]

Low current and as small as several micro gap discharges behaved as a normal discharge. Micro size discharge has been used in plasma TV, display panel, material processing, fabricating polymer/ metal, and analytical instrument etc.[18]

2.3.3 Dielectric barrier discharge DBD

Using dielectric material in between the discharge gap keeps from large current and stop spark formation. DBD (as shown in figure 5) has its strong non-equilibrium characteristics and widely used in applications. The first DBD device invented by W. Siemens in 1875 used for ozone generation and proposed the name ‘‘silent discharge’’.

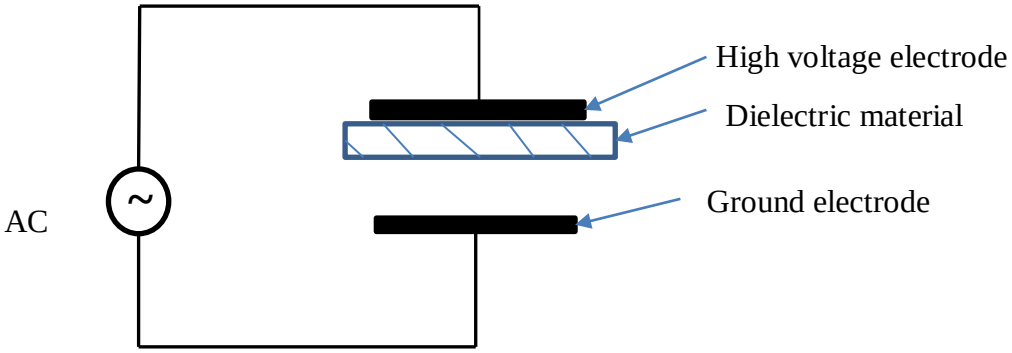

Figure 5. Dielectric-barrier discharge configurations

High frequencies current will fail the dielectric barrier and develop to large current. Thus, for this reason DBDs are normally operated between line frequency and about 10 MHz. The numerous micro-discharge breakdown are observed at atmospheric pressure

This pressure is benefit ozone generation, gas treatment and pollution control. Discharge gap varied form 0.1mm to several centimeters while voltages in the range of a

few hundred V to several kV are required.[19] Surface modification, plasma chemical vapor deposition, pollution control, excitation of CO_2 lasers and excimer lamps and, most recently, in large-area flat plasma display panels used in wall-hung or ceiling attached television sets.

2.4 Literature review

Different oxidizing feedstock have been used in plasma reforming: 1) dry reforming (CO_2)[9, 20, 21], 2) partial reforming (air)[22], 3) steam reforming (H_2O) [23, 24], 4) modified partial oxidation (air/water)[25, 26]. Various atmospheric discharge techniques, such as pulsed corona, dielectric barrier discharge (DBDs), micro discharges, gliding arc discharges and magnetic glow discharges have been applied for conversion of methane.

Table 3, presents a summary of the results and data presented in reference was converted to common units for comparison. The parameters are hydrocarbon flow rate, discharge power, methane conversion rate, H_2 selectivity, CO selectivity.

Focus on mainly promising types of discharges: Dielectric Barrier Dischargers (DBDs), corona, microwave and glow. In several studies, with catalyst + plasma processes offer more selectivity and higher conversion rate than without catalyst, but they need to be operated at higher temperature, a certain gas composition and strict control to keep active catalyst and avoid losing active. [25]

The gliding arc to accelerate chemical reaction at low temperature with very low energetic costs, 44 MJ/kg H_2 was reached with around 450W power input at CH_4/H_2O=

4, while larger amount of acetylene(up to 1%) were also evidenced, and the condensed unreacted water contained a depot of carbon black [27]. And others like raw natural gas (contain 20% CO_2) reforming under AC gliding arc discharge, got around 20% methane conversion, 70% H_2 selectivity and relatively low power consumptions.[20]

A corona inducing DBD reactor was investigated with feed gases: air, methane and steam (54%, 23% and 23% respectively). At 0.35 slpm methane and 50W power input at 200 ºC reached 50% methane conversion and 105% hydrogen selectivity [28]. Fridman team used a pulsed corona discharge reactor with preheated inlet gas at about 900 ºC[20]. They succeeded in lowering the plasma energy cost to 34 MJ/kg H_2. However, the energy spent for preheating the mixture was about 340 MJ /kg H_2. [27]

The microwave plasma can have a higher energy density and higher ratio of electron temperature to ion temperature than pulsed corona discharge. Wang etc al reached 91.6% conversion rate with as low as 13.8 eV/molecule specific energy of H_2, in 90% nitrogen, CH_4/H_2O= 1 at 1.0 kW, and 12slpm.[24]

A system response was achieved at inputs of 2 slpm N_2, 0.56 slpm O_2, 1.25 slpm CH_4, 0.6 g steam/min, an electrode gap distance of 34.5 mm, and a power input of 260 W. After water separation, the reformate produced under these conditions was comprised of 35.5% hydrogen, 0.2% oxygen, 16.6% carbon monoxide, 1.4% carbon dioxide and 5.7% methane. The post-reaction chamber temperature remained at a steady temperature of 271 ºC. At this point, hydrogen selectivity was 83.3%, methane conversion 79.8%, a specific energy requirement of 77 MJ/kg of hydrogen produced. [29]

Table 3. Literature review data

Discharge type		Flow rate of hydrocarbon slpm	Power (W)	Temperature (ºC)	Methane Conversion rate (%)	CO Selectivity(%)	Hydrogen Selectivity(%)
DR	Pulsed corona [20]	1.25	10	900	14.80%	45.96%	48.64%
SR	DBD [23]	0.33	200	200	17.30%	30.20%	38%
SR	Microwave plasma [24]	0.6	1000	>750	91.60%	NA	95.20%
POX+SR	DBD [25]	0.12	30	400	28%	58%	32%
POR+SR	Gliding Arc [26]	0.72	14.5kV	120	NA	59.90%	68.20%
POX+SR	DBD /NiO [28] a	0.35	50	<600	50%	NA	105%
POX+SR	Vertex Arc [29]	1.25	260	271	NA	16.60%	83.30%
SR	DBD Ni/SiO_2 [30]	0.0108	275	500	50%	45%	NA
SR	DBD [31]	0.033<	15.3	600	13%	34%	53%
DR	Pulsed glow and arc [32]	0.06	23	70	61%	65%	77%

a: fuel content of 70% methane, 5% ethane, 5% propane, 20% CO_2

POX: partial oxidation

SR: steam reforming

DR: dry reforming

3. EXPERIMENTAL APPARATUS AND PROCEDURE

3.1 Reactor system

Rotating glow discharge system is one of non-thermal equilibrium plasma with slightly high gas temperature. This reactor system is operated under continuous flow, atmospheric pressure and a range of temperature ($120 \pm 10℃$). Glow discharge was generated between stainless steel tube and rod, and tube and rod aligned axially. Uniform magnetic field applied perpendicularly on discharge, which kept glow discharge spinning. Feed gas would be premixed and warmed up, and went through uniform rotating glow discharge. Requirement of system:

1. Glow discharge current in the range of 30mA to 80mA
2. Heat up system avoids steam to condensing. Thermo heater tape rolled on feed in gas line ,wrapped with insulation material glass wood
3. High strength magnetic field to maintain uniform rotating discharge at maximum flow rate and abnormal situation, ex. carbon formed on electrode and hot spot
4. Visibility of discharge and Discharge stability
5. Material used for electrode should stand high temperature
6. Controllable feed in flow rate

As shown in Figure 6, 7, and 8, the reactor setup configuration of hydrocarbon gas reforming, ammonia synthesis, and experimental reactor and accessories.

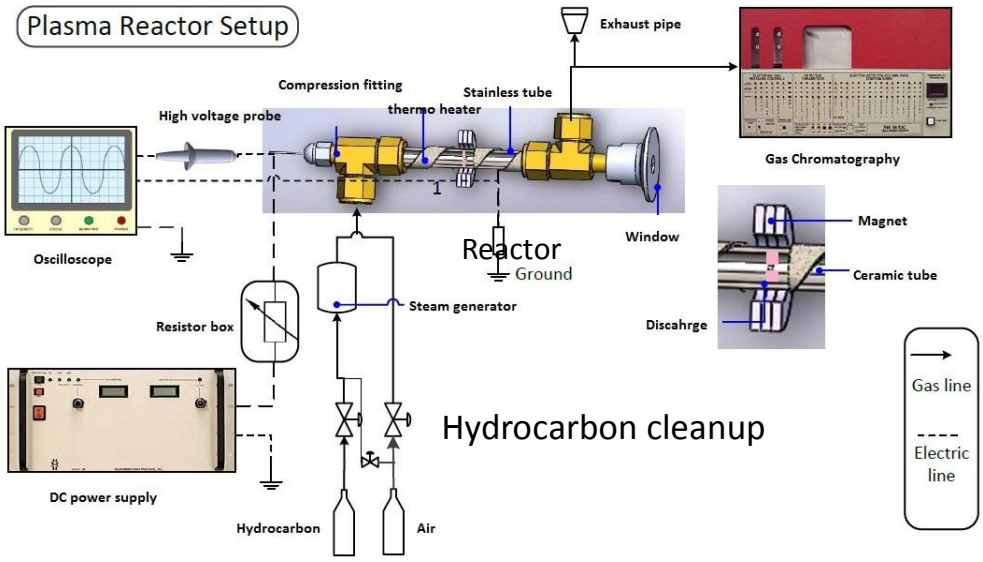

Figure 6. Hydrocarbon clean up setup configuration

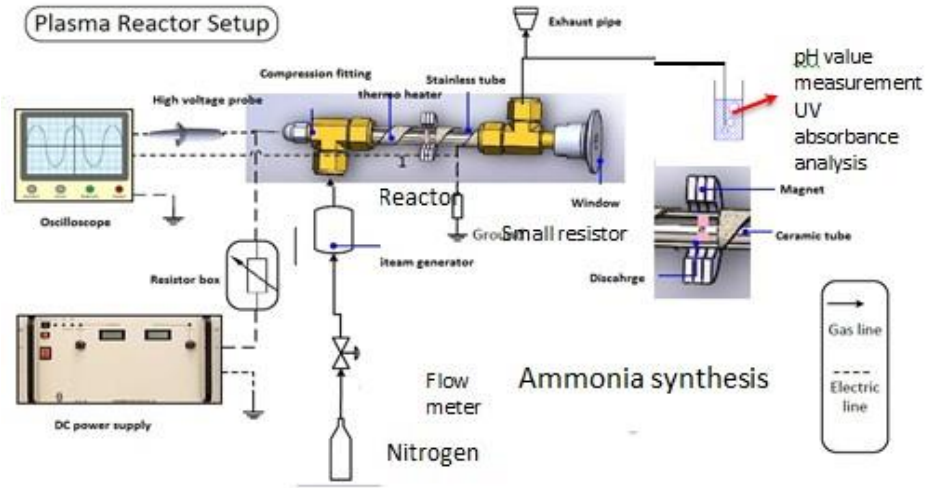

Figure 7. Ammonia synthesis setup configuration

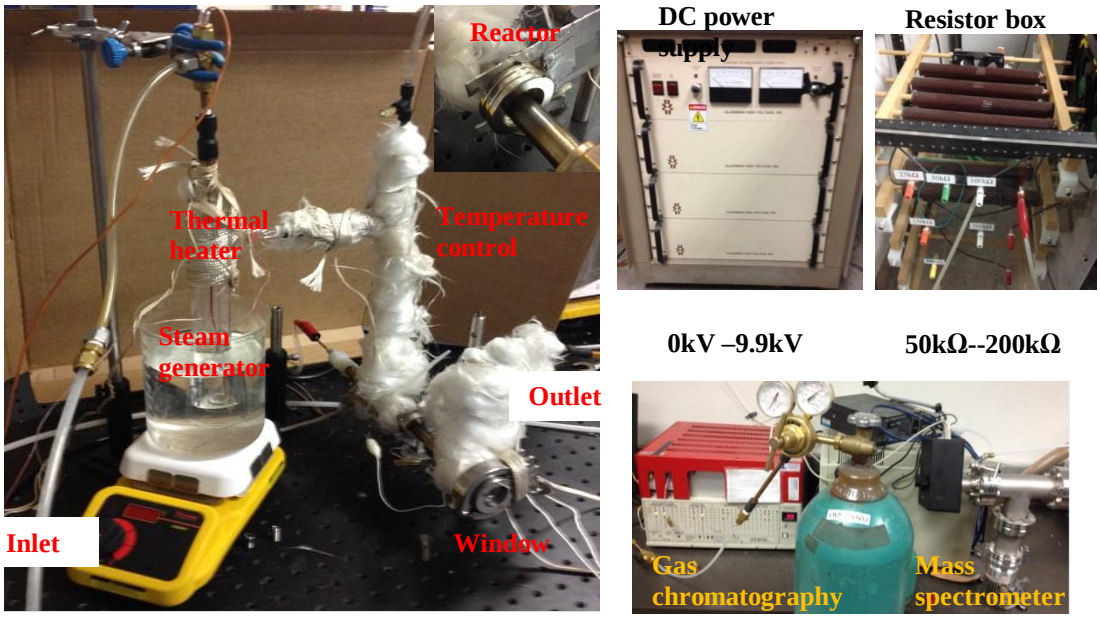

Figure 8. Reactor setup

3.2 Experimental setup

Stainless steel tube, outside diameter (OD) 1/2" & inside diameter (ID) 0.40", worked as ground and coaxed 1/8" inches stainless steel rod as high voltage. Stainless steel rod was covered by alumina ceramic tube. The discharge gap was 0.15 inches and the length of discharge was 2 mm in figure 9. Outside of stainless tube was coaxial with 1/4" OD x 3/4" ID x 1/8" thickness K&J ring-shape magnets. The magnetic field visualization single magnet in free space showed in figure 10.

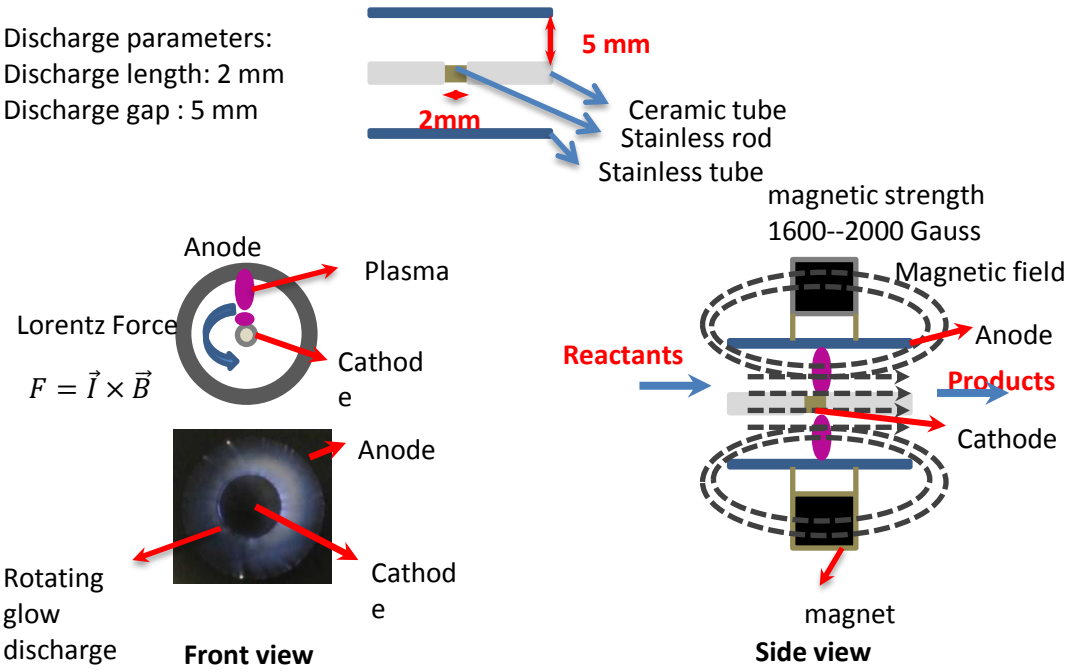

Figure 9. Configuration of discharge

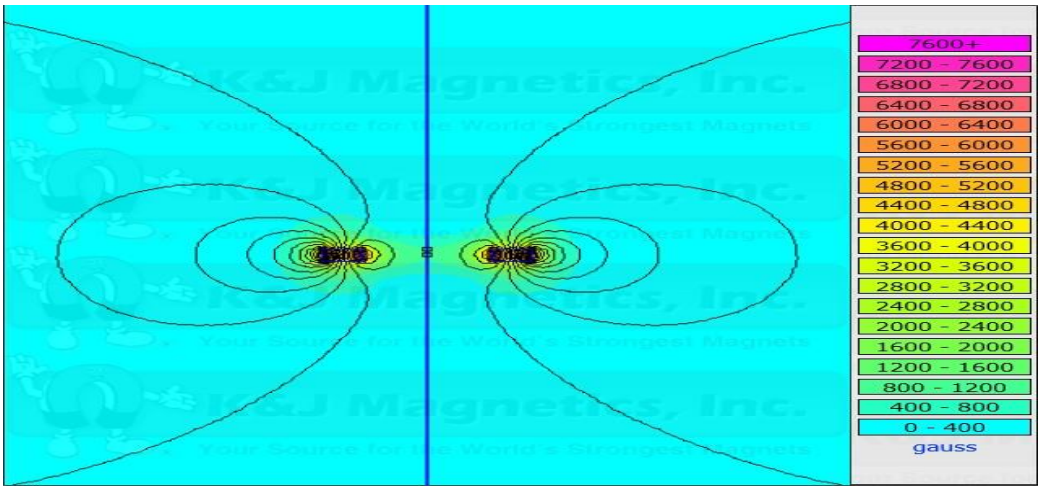

Figure 10. The magnetic field visualization single magnet in free space [33]

The average magnetic strength single magnet applied on plasma is 1600--2000 Gauss as shown in figure 10. Connected with fitting compressor and cord grip and window, the whole reactor rolled with thermal heater and insulated by glass wool. The whole setup for ammonia generation and hydrocarbon gases cleanup, was shown in figure 6, 7, and 8.

3.2.1 Steam generator

Steam generator system was used to produce steam including steam generator, 1000ml beaker, maximum 540 ºC heat plate, thermo heater, K type thermo couples, glass wood, etc. Stream generator body was bathed in hot water (temperature varied from 45℃ to 95℃ in order to contral steam concentration in feed gas). As showed in the figure 11, two thermocouples, added on steam generator, help to control steam concentration through holding different temperature of bath water. K type thermocouple 1, inserted at the bottom of in the steam generator, measured the temperature of stilled water. The body part of steam generator bathed in hot water, and other part in air rolled with thermo heater and wrapped with glass wood, avoiding steam condensation and preheating the inlet gas. Another K type thermocouple 2, added at outlet part of steam generator, measured the temperature keeping steam from low temperature and condensation.

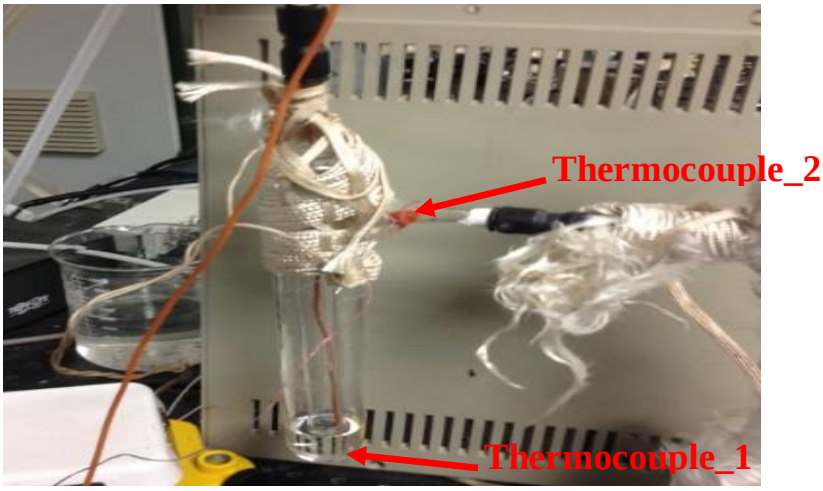

Figure 11. Bubbler and thermal couples

Primarily, in order to figure out H_2O/gas ratio of feed mixed gas at different bath temperature, industrial grade nitrogen (N_2 99.95%) was used as carrier gas in test. Nitrogen flowed into inside glass tube, and warmed up and bubbled through distilled water. By measuring at different bath temperature distilled water consumed, total time nitrogen bubbled through it and flow rate of nitrogen gas, then got the H_2O/gas ratio for different bath temperature show in figure 12. This figure roughly helped to indicate H_2O/gas ratio, which was easily to figure out what H_2O/gas ratio I can get at a temperature range. However, each individual experiment had different H_2O/gas ratios. In additionally, distilled water consumed defined as the difference mass of steam generator Δm before and after bubbling, the bubbling time varied from 30 to 60 mins.

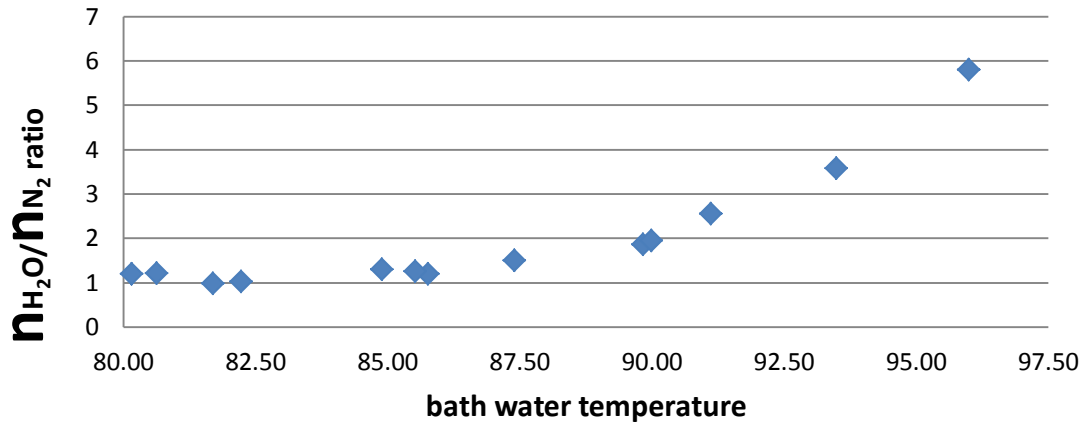

Figure 12. Water/nitrogen ratio at different bath temperature

3.2.2 Flow line

EPE flow line

Industrial grade EPE gas (74.8% methane, 8% ethane, 8% ethylene, 4% carbon dioxide, 2.1% propylene, 1.1% propane, 2% hydrogen) controlled by ALICAT scientific flow controller and compressed air regulated via volumetric flow rate by ALICAT scientific flow controller. EPE gas and air bubbled through and mixed in steam generator, taking with steam. Then hot air, steam and EPE gas mixture kept warm and went through plasma discharge. Products flowed out of chamber and went through condenser. After removed water, products were collected by syringe for gas chromatography analysis and rest of them flowed to exhaust line.

Ammonia flow line

Industrial grade nitrogen (99.9%) controlled by ALICAT scientific flow controller. Nitrogen bubbled through steam generator, taking with steam. Then steam and nitrogen mixture kept warm and went through plasma discharge. Products flowed out of chamber and went through condenser. After removed water, products were conducted to mass spectrometer analysis and rest of them flowed to exhaust line.

3.2.3 Power line

A DC power supply, a range from 0 kV to 9.9 kV, provided power source to plasma discharge. The maximum current limit was 250 mA. DC power supply generated negative high voltage, and connected with ballast resistor box with 50 kΩ, 100 kΩ, 150 kΩ and 200 kΩ. The ballast resistor helped to stable current. High voltage line connected with stainless rod, while stainless tube was connected with a small resistor (10 Ω) for current measurement on oscilloscope, and then ground.

3.2.4 Chromatography and mass spectrometer

After removed water in products, used syringe to collect the products and injected in SRI 8610C gas chromatography (GC). The GC connected with Extorr mass spectrometer (MS). A 6 inches molecular sieve column and a 6 inches silica gel column equipped on GC to separate compositions of product gases. Molecular Sieve column used to separate hydrogen, oxygen, nitrogen, carbon monoxide and methane. Silica Gel column performed better separation in hydrocarbons and carbon dioxide than Hayesep D column. Two detectors installed to detect those gases. Helium ionization detector and

thermal conductivity detector had sensitivity of concentration 50ppm and 1%, respectively.

3.2.5 UV-VIS spectrometer

In ammonia solution analysis, UV-VIS TE Cooled CCD Spectrometer was used. Its wavelength range are from 200 nm to 800nm, resolution is 1.5 nm, slit width 25 µm. as shown in figure 13.

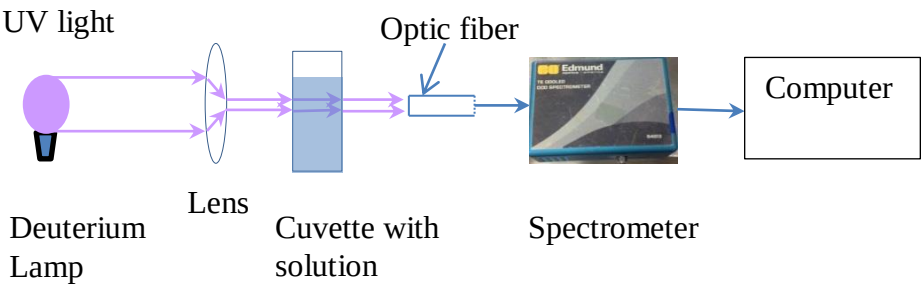

Figure 13. UV light absorbance analysis setup

4. DIAGNOSTICS TECHNIQUES AND ANALYSIS METHODS

4.1 Voltage and current

Plasma power, or the discharge power, is defined as energy spend on discharge reactor system to converting initiate chemical reaction and corresponding products, Some energy losing into heating up gases and the reactor.

Power on plasma is measured using oscilloscope (Lecroy Wave Runner 204 MXi). The measurement is design to keep accuracy as high as possible. Plasma power in other words is power measured at negative high voltage electrode. Current sensing resistor was integrated into circuit in order to obtain discharge current as shown in figure 14.

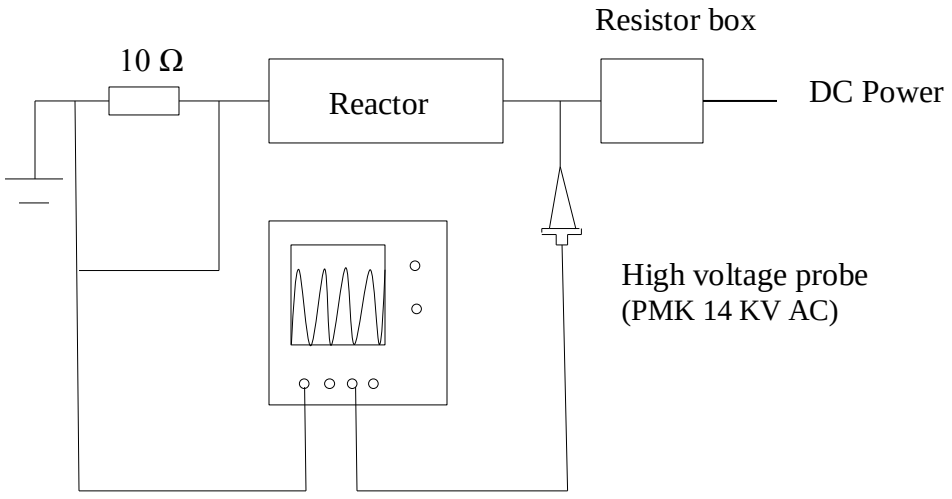

Figure 14. Plasma power measurements

4.2 Mass spectrometer

The XT Residual Gas Analyzer (RGA) from Extorr, A Faraday cup detector is standard with 100 amu systems. The ultra-sensitive, wide dynamic range amplifier detects ion currents from 10^{-6} to 10^{-15} Amps automatically. This allows partial pressure measurements from 10^{-4} to 10^{-11}Torr. [34] Mass spectrometer was connected with vacuum pump in order work at vacuum condition. This vacuum pump provided 10^{-4} to 10^{-6} Torr work pressure for mass spectrometer as shown in figure 15.

Figure 15. Mass spectrometer and vacuum pump

4.3 Gas chromatography

SRI 8600C Multiple Gas Analyzer GC, as shown in figure 16, is pre-plumbed and ready to resolve H_2, O_2, N_2, Methane, CO, Ethane, CO_2, Ethylene, NO_x, Propene, Acetylene, Propane, Butanes, Pentanes, and C_6 through C_8. A GC is consisted of Heated valve oven, 10-port gas sampling valve and 1mL sample loop, Sample IN and OUT, On-column injector, Temperature programmable column oven, TCD detector, 6' Molecular Sieve, 6' Silica Gel , TCD detector, HID detector.

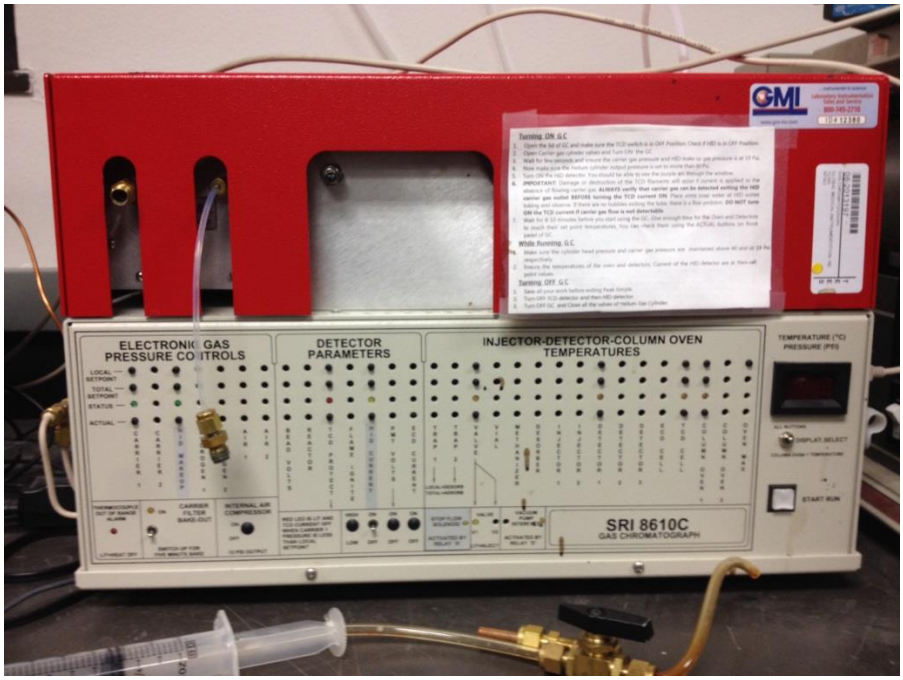

Figure 16. SRI 8600C multiple gas analyzer GC

The Helium Ionization Detector is a universal detector, responding to all molecules except neon. It requires only helium carrier and make-up gas, and is sensitive to the low ppm range. The HID is particularly useful for volatile inorganics to which the FID and other selective detectors will not respond, like NO_x, CO, CO_2, O_2, N_2, H_2S and H_2. It is a robust detector that, unlike the TCD, has no filaments to burn out. The SRI HID consists of a detector body, a collector electrode, an arc electrode assembly, and a thermostatted heater block which can be heated to 375ºC. In SRI GCs, the HID is mounted on the right-hand side of the Column Oven.

The SRI HID detector uses two electrodes which support a low current arc through the helium make-up gas flow. The helium molecules between the electrodes are elevated from ground state to form a helium plasma cloud. As the helium molecules collapse back to ground state, they give off a photon. The sample molecules are ionized when they collide with these photons. All compounds having an ionization potential lower than 17.7eV are ionized upon contact with photons from the helium cloud. The ionized component molecules are then attracted to a collector electrode, amplified, and output to the PeakSimple data system.

The Thermal Conductivity Detector (TCD) is the most universal detector available. Depending on the compound, the TCD responds with a detection range of 0.01% to 100% (100-1,000,000ppm). The SRI TCD consists of four filaments housed in a stainless steel detector block. The TCD detector block is installed in its own thermostatically-controlled oven for stability. The TCD oven is mounted on the right

rear of the column oven. The TCD filament control switch and the bridge terminal block to which the filament leads are connected are located to the immediate right of the detector oven. Since the four TCD filaments can be damaged or destroyed if energized in the absence of carrier gas flow, a TCD filament protection circuit is provided in all TCD-equipped SRI GCs.

The TCD detector measures the difference in thermal conductivity in the carrier gas flow and the analyte peaks. Every compound possesses some degree of thermal conductivity, and may therefore be measured with a TCD detector. Due to its high thermal conductivity and safety, helium carrier is most often used with TCD detectors. However, other gases may be used such as nitrogen, argon, or hydrogen

A one-milliliter sample loop is connected to the 10-port gas sampling valve. When the valve is in the LOAD position, sample may be flowed through this loop until the moment injection occurs (when the valve switches to the INJECT position) as shown in figure 17.

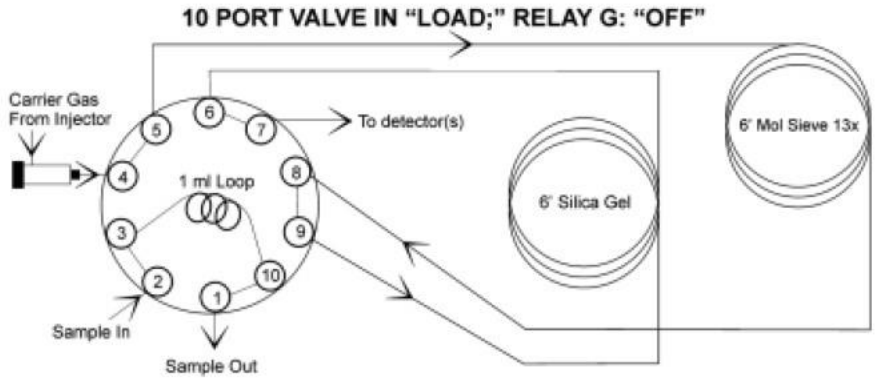

Figure 17. Valve is in the LOAD position [35]

At the beginning of the chromatographic run, the valve is actuated to the INJECT position as shown in figure 18, depositing the sample loop contents into the carrier gas stream and directing it to the two analytical columns, which are connected in series through the 10-port valve.

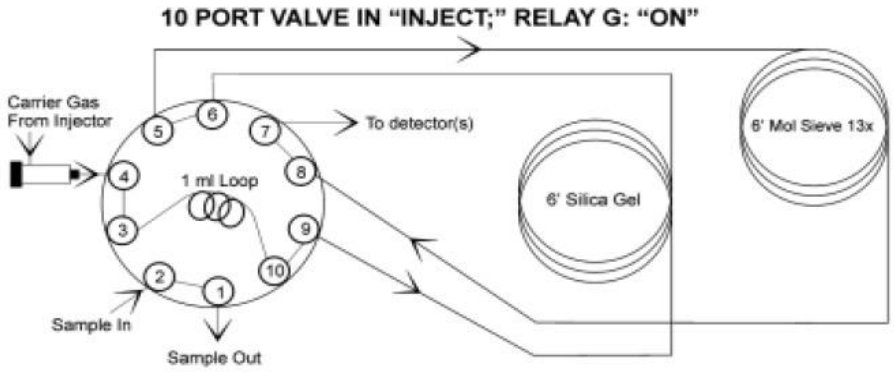

Figure 18. Valve switches to the INJECT position [35]

The sample is deposited by the carrier gas stream first into the Silica Gel column, with the column oven holding at 40 ºC, where the ethane, propane, butanes, pentanes, and carbon dioxide are retained. The remainder of the sample containing H_2 (or helium, whichever is not being used as a carrier), O_2, N_2, methane, and CO, continues on to the Molecular Sieve column. During a chromatographic run with the sampling valve in the INJECT position, the H_2 or helium, O_2, N_2, and methane components are the first to elute through the columns and into the detector. This is due to the Silica Gel's long retention of C_2, CO_2 and higher hydrocarbons at 40 ºC. The sampling valve is actuated back into the LOAD position immediately following the elution of the CO peak. This reverses the sequence of the columns prior to the detector, and sends the components preparing to elute from the Silica Gel packed column (ethane, propane, etc.) to the detector without passing them through the Molecular Sieve packed column. At the same time, the Silica Gel packed column is temperature 20 ºC/min ramped to 160 ºC promote the rapid elution of the remaining components. [35] Program steps including Event & Temperature, and species eluting time listed in Appendix.

4.3.1 Sample collecting

Product gas composition analyzed by SRI made gas chromatography. A special lab made syringe was used to collect sample. This lab-made syringe resolved the noise come from air, totally cleaned up air. As shown in figure 19 a), Flow comes in one end and comes out another end. The traditional syringe meets a difficulty to clean up air in tube part as shown in figure 19 b).

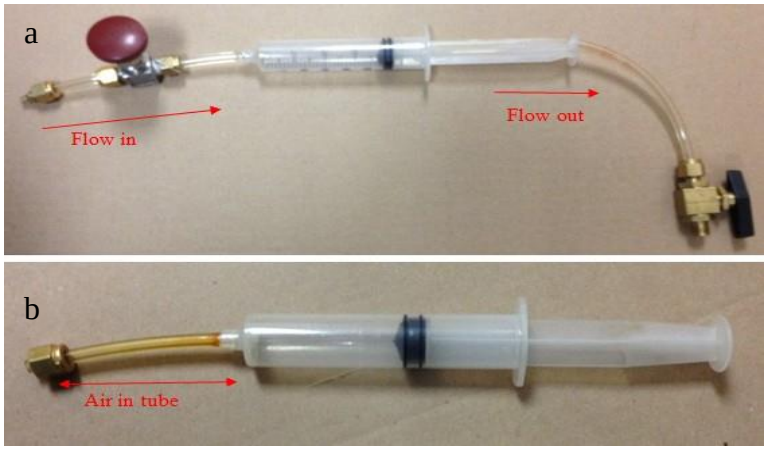

Figure 19. a) Lab-made sample collector, b) traditional sample collector

If air was participate reaction as an oxidizer, coming in extra air in sample collecting will generate uncertainty, and result in inaccuracy on experimental data. As shown in figure 20 a), showed the result of EPE gas calibration was taken form lab-made syringe sample collector. It's very clearly that there was no air be detected. Meanwhile, figure 20 b) showed that around 2%-5% air mixed in sample. Due to the tube part of sample collector, it's impossible to evacuate all the air out. Even though take several times to repeat the evacuation process, there is still air inside sample collector. The lab-made sample collector has flow in end and out end, which means it does need to do the evacuate process. The sample gas will flow into and swap the air out from another end. This process will take 30 seconds to 1 minute clean up all the air out and then close these two valves. Then the taking sample process finished.

a

b

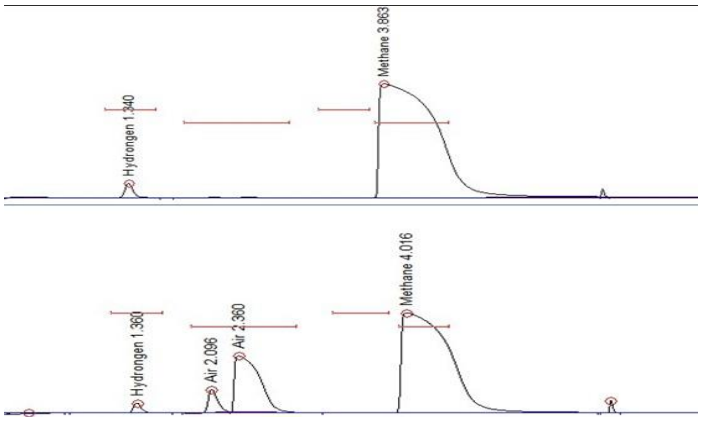

Figure 20. a) Lab-made sample collector GC plot, b) traditional sample collector GC plot

The detail of sample process: hot products steam flow into steam condenser and cool down. After removed water, product gas went on flowing into water collecting chamber and then flow to exhaust pipe. Without collecting gas sample, only valve 1 was open and other valves closed. When need to collect the gas sample, the syringe was ready at load position. The valve 1 was closed and valve 2, 3 and, 4 were open. After 30 seconds, closed valve 4 and slowly took sample in syringe. Then open valve 4, let the flow went through syringe for a while. Last close valve 2, 3, and 4, reopen valve 1 and take the syringe off, as shown in figure 21.

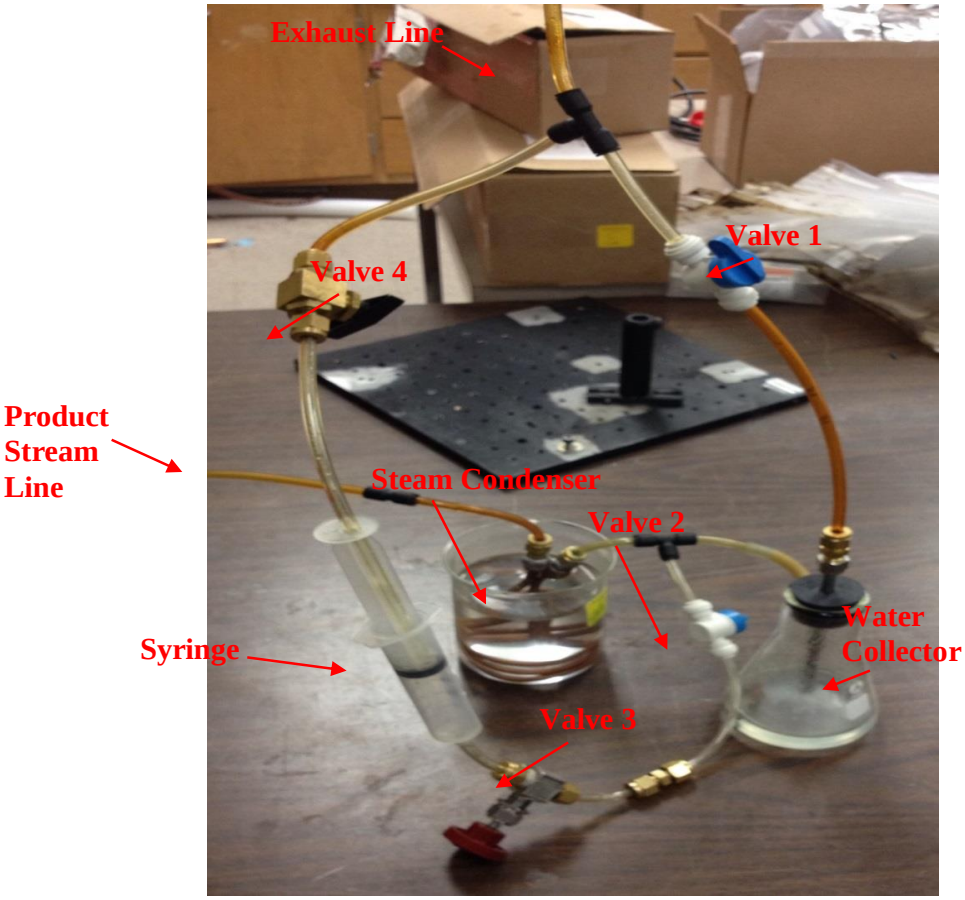

Figure 21. Sample collection setup and water remove setup

4.3.2 Calibration

Gas chromatography calibration is a comparison between measurements – one of known magnitude (correct percentage of each gradient) and another measurement made in as similar a way as possible on GC. The known percentage of gradient of gas already settled is called the standard. The gas chromatography measurement is the test instrument, or any of several other names for the GC being calibrated. Once the GC was calibrated, the environmental set-up should be keep the same, the helium pressure, heating temperature, and ramping temperature etc. Besides, in order to maintain gas chromatography accuracy, it required to calibrate GC very one month and a long period shut down.

The calibration process was EPE gas calibration, carbon monoxide calibration, and acetylene calibration. EPE gas contain (74.8% methane, 8% ethane, 8% ethylene, 4% carbon dioxide, 2.1% propane, and 2% hydrogen, 1.1% propene). Carbon monoxide calibration measure 5%, 10%, 20%, and 30%, balanced with hydrogen. Acetylene calibration, bought Air Liquide analysis gases, (5% acetylene, 4.99% ethane, 4.98% ethylene, and balanced by nitrogen). A standard temperature should run on GC and also multiple times to avoid errors. Generally, gas chromatography connected with mass spectrometer to help identify what it comes up on gas chromatography. Acetylene and EPE as an example on mass spectrometer was shown in figure 22, 23 and 24.

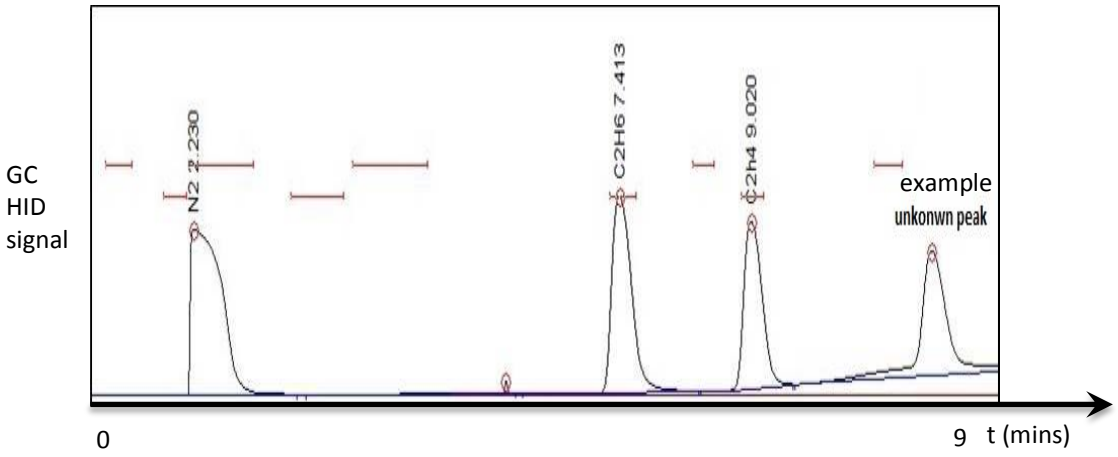

Figure 22. Acetylene GC peak

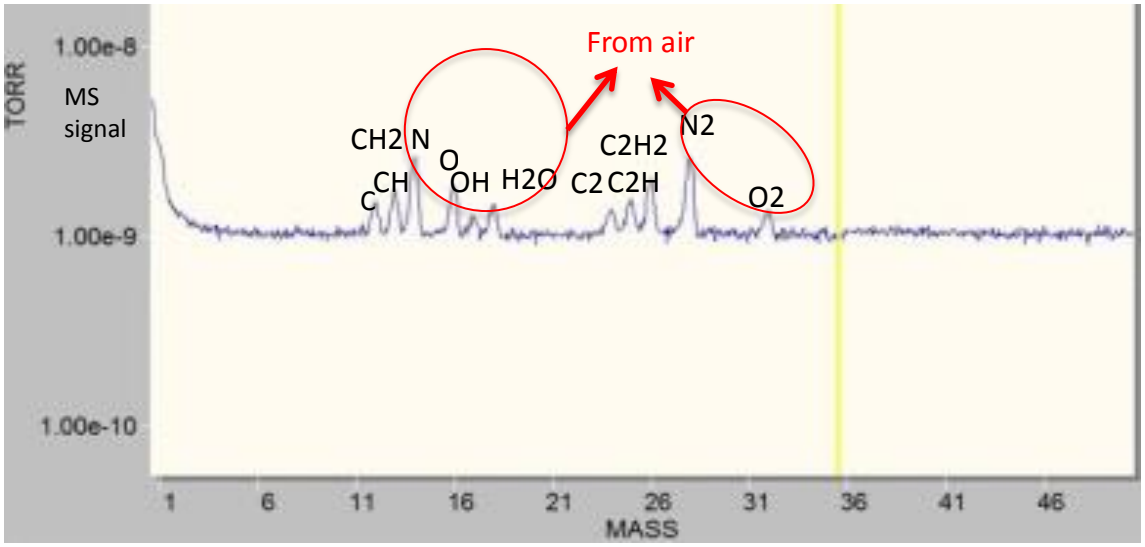

Figure 23. Acetylene on mass spectrometer

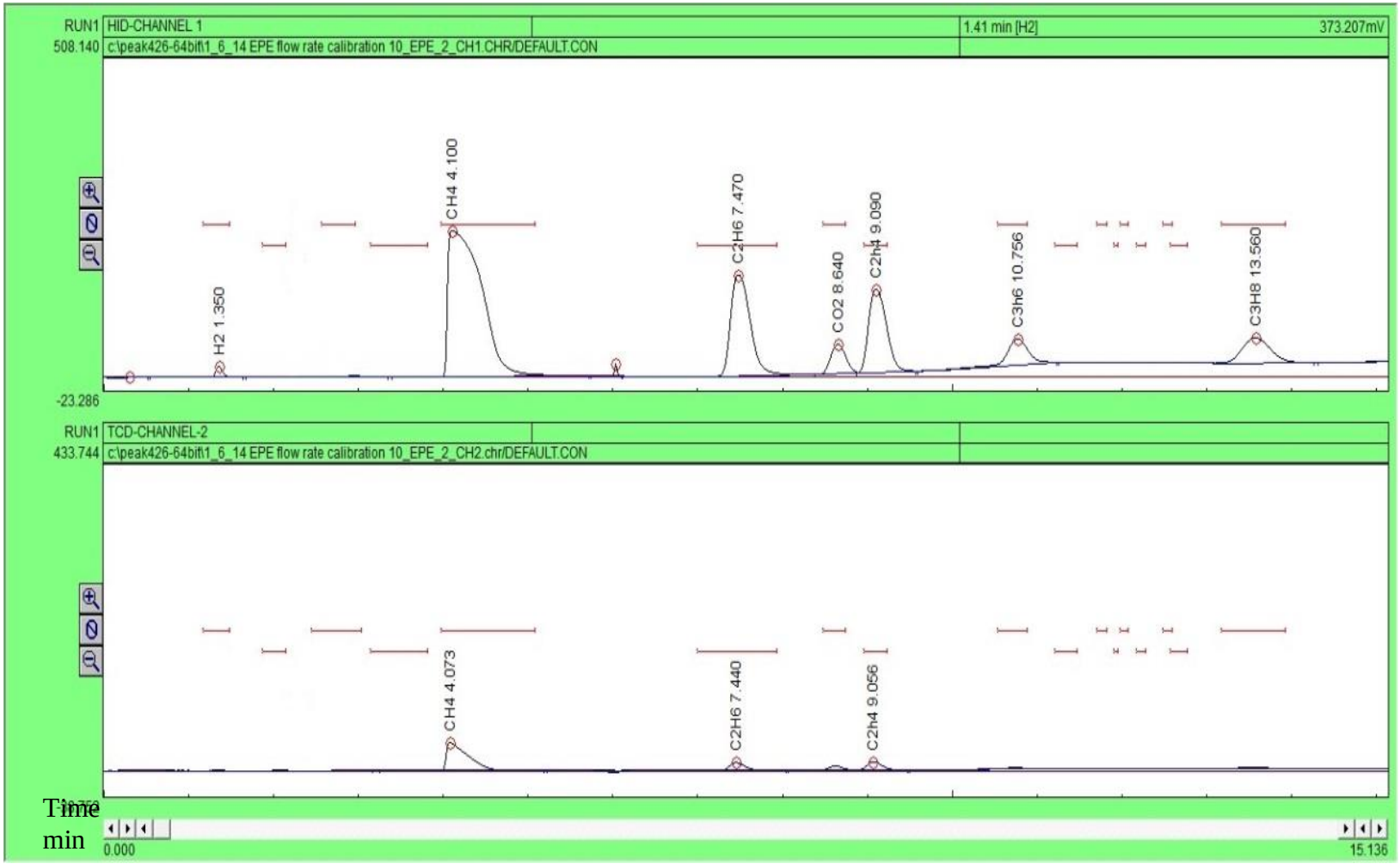

Figure 24. Calibration of EPE gas

4.4 Ultra violet absorbance diagnostic setup

The feed-in gas mixture was then introduced into the rotating glow discharge reactor. After plasma treatment, gaseous products bubbled in pure water and the solution was analyzed by UV-VIS spectroscopy. UV light analysis setup as shown in figure 25, Use deuterium lamp generated UV light went through focus lens and formed a UV light beam through quartz cuvette with solution. The output light collected by optic fiber and went through UV-VIS TE Cooled CCD Spectrometer, and then sent the signal to computer. All the process was conducted in dark room, and did one cuvette with solution and another one cuvette without solution in order to subtract the noise from surrounding environment. Absorbance A_λ is a quantitative measure expressed as a logarithmic ratio between the radiation falling upon a material I_1 and the radiation transmitted through a material I_0. $A_\lambda = -log\frac{I_1}{I_0}$

$$A_{\lambda\ ammonia} = A_{\lambda\ cuvette\ without\ solution} - A_{\lambda\ cuvette\ with\ solution}$$

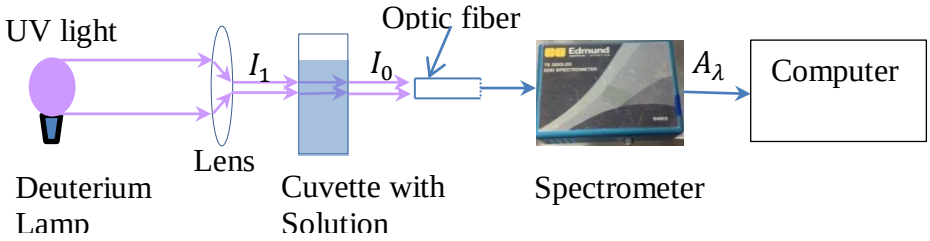

Figure 25. UV light absorbance

4.5 Bromothymol blue(BTB) diagnostic setup

In this experiment, Bromothymol Blue(BTB) was used as pH value indicator for weak acids and bases solution. It will show yellow as soon as pH below 6. When pH value is between 6 and 7.8, green color will be observed as shown in figure 26. As soon as the pH value is greater than 7.8, it will totally transfer from green to blue. Bromothymol Blue solution is an ideal pH indicator when small amount ammonia was generated.

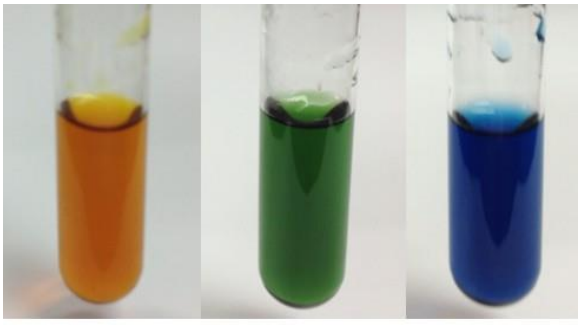

Figure 26. Bromothymol blue colors in different range of pH value

5. RESULTS AND DISCUSSION

5.1 Ammonia synthesis

Nitrogen got through bubbler and carried water vapor at room temperature. As feed-in gas with low humidity at room temperature and treated in plasma, product stream bubble through was observed and the bromothymol blue(BTB) show blue. In figure 27, showed hue value changed with time, varied from green to blue. Also the pH value change with time.

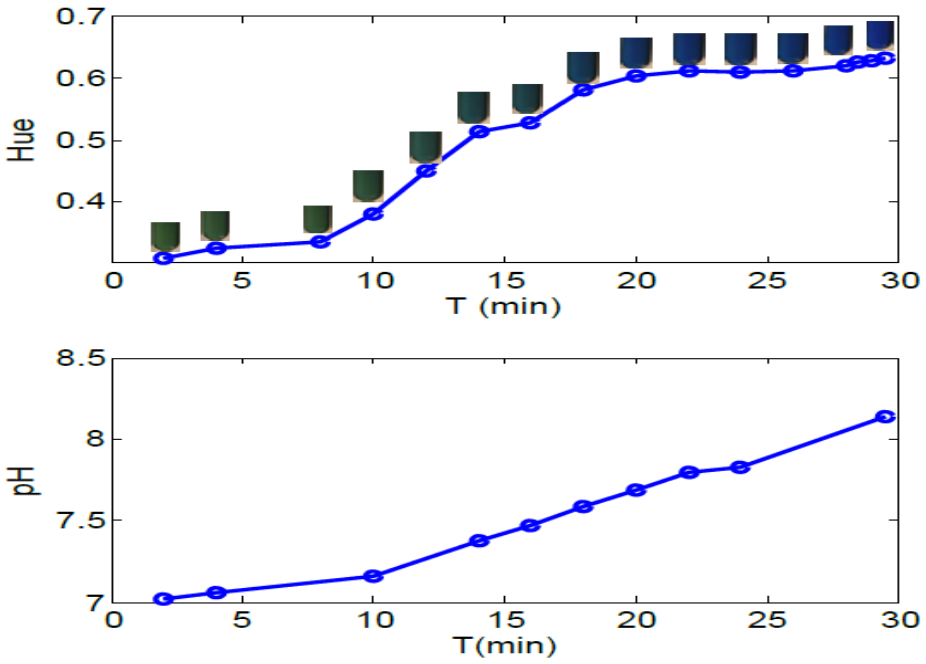

Figure 27. Nitrogen flow rate 67.4 ml/min; Power 30 W, BTB 18.4 ml at room temperature

In order to use UV-VIS to analyze, product gas bubbled through distilled water as UV-VIS test solution. All products stream was bubbled into 3 ml distilled water in 10 mins at 30W power and 50% nitrogen and 50% steam tested by UV-VIS spectroscopy in figure 28. The normalized absorbance peak is at 217.61nm compared with 216.8 from A.D. Walsh[36].

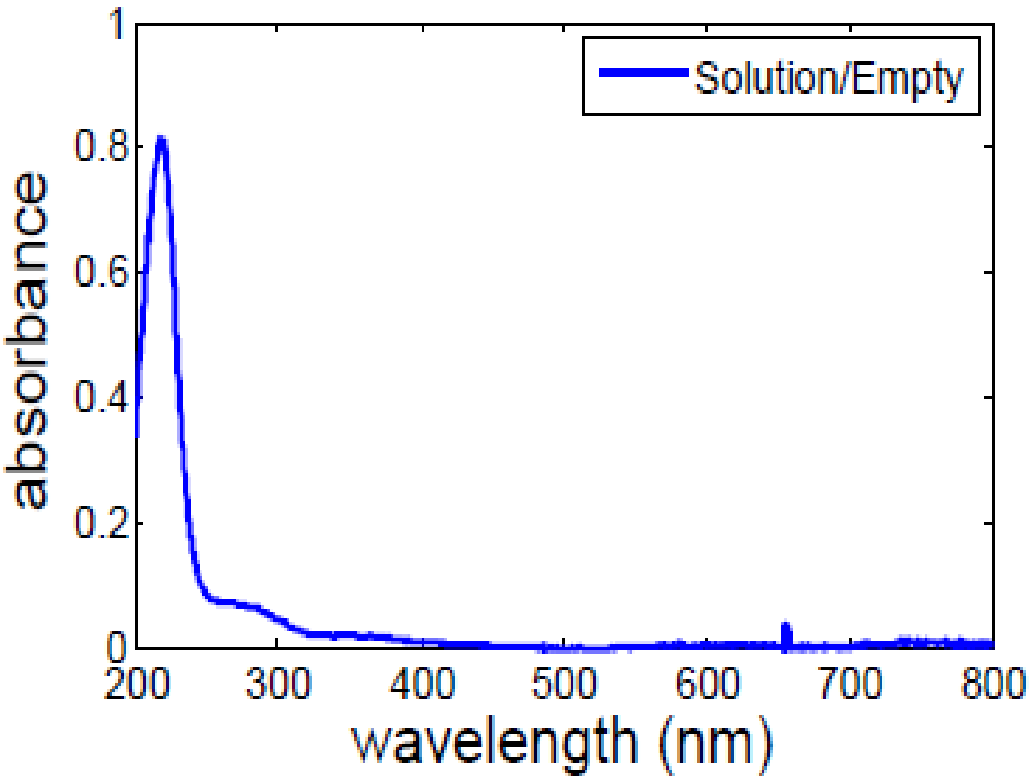

Figure 28. Ammonia absorbance wavelength

5.2 EPE gas cleanup

5.2.1 Measurement methods of involving variants

These parameters are defined below

1. Output stream volumetric flow rate $\dot{V}_{out}$:

In this experiment, a known volumetric velocity inter gas$\dot{V}_{in_{N_2}}$, nitrogen, was used to measure the output stream volumetric velocity. Mole fraction of nitrogen in output stream was measured by GC $X_{out_{N_2}}$

Output stream volumetric flow rate defined as:

$$\dot{V}_{out} = \frac{\dot{V}_{in_{N2}}}{X_{out_{N2}}}[\text{sccm}]$$

2. Specific energy [MJ/kg]or [eV/molecule]:

energy spent on per Kg reactant or product gas. Specific energy input on product is given as

$$E_i = \frac{60}{\rho_i} \times \frac{P}{\dot{V}_i} \times 10^{-6}[\text{MJ/Kg}]$$

Where:

i represent species of products or reactants (hydrogen, Carbon monoxide etc.)

E_i [MJ/kg]Specific energy input on i reactant or product

$\dot{V}_i = \dot{V}_t \times X_i$ [sccm] i species' flow rate

$\dot{V}_t$ [sccm] total output flow rate

X_i [%] mole fraction in output stream

ρ_i [kg/cm^3]i species' room temperature and atmospheric pressure density

P [W]power input at discharge

Converting [MJ/kg] to [eV/molecule]:

$$E_i[\text{eV/molecule}] = [\frac{10^6 \times M_i}{e \times Na}] \times E_i[\frac{MJ}{kg}]$$

Where:

e is conversion factor for eV to joules

$1\ eV = 1.602 \times 10^{-19}\ joules$

$Na = 6.022 \times 10^{26}\ kmol^{-1}$

$M_i[kg/kmol]$ molecular weight of i species reactant or product

3. Conversion rate [%]:

Conversion described as ratios how much of a reactant has been reacted or being converted into products.

Converted hydrocarbon can be calculated in this way:

Hydrocarbon conversion defined as:

$$C_nH_m[\%] = 1 - \frac{X_{CnHm_{in}}\dot{V}_{in}}{X_{CnHm_{out}}\dot{V}_{out}}[\%]$$

4. Selectivity[%]:

How much desired product was formed in ratio to the whole products.

EPE gas reforming resulting in variety of products mainly are hydrogen, carbon monoxide, carbon dioxide (depends on water/EPE ratio) and trace of acetylene. The ratio of certain product to total conversion EPE gas gives selectivity of this certain product.

$$S_i = \frac{n_i}{n_{total\ converted}} \times 100\%$$

Where:

S_i selectivity of products

n_i ith mole of product

n_{total} total mole product

5. Flow residence time

Flow residence time is a term that described reactants spent on discharge or exposed to plasma discharge. In this work, residence time was defined as flow residence time in which input stream gas impacted by energetic electron and generated radicals, the initiating chemistry in short and then quickly quenched. The duration of flow residence time influenced on generating radicals and chemistry which subsequently lead to end products.

$$\tau = \frac{\pi r^2 \times L}{\dot{V}}$$

Where:

τ is flow residence time

r radius of tube

L length of discharge

$\dot{V}$ volumetric flow rate

6. Process Efficiency [%]

Efficiency described how much energy stored in products in term of the ratio of product enthalpy to total energy used to reforming. Ideally, energy spent on reforming EPE gas transfer into products without any type of energy loss.

Hence the efficiency for whole reactor system was give as

$$ŋ = \frac{n_p \sum LHV_p}{n_i \sum LHV_i + W} \times 100\%$$

Where

ŋ efficiency of system

n_p mole of ith products

LHV_p low heating value of ith products

n_i mole of ith reactant

LHV_i low heating value of ith reactant

W electric input energy on plasma

7. Feasibility [%]

Feasibility is defined as a ratio between plasma power and electricity generated by treated product. This term describe systems sustenance when feasibility less than 100% or not self-sustainable when it great than 100%. In order to output electricity, the feasibility should be the small the better. Fuel cell efficiency taken as 0.5 [8].

$$\text{Feasibility } = \frac{\text{Plasma Power}}{(\text{product LHV}) * (\text{fuel cell efficiency})} * 100\%$$

$$\theta = \frac{P}{n_p \sum LHV_p * \mu} \times 100\%$$

Where

θ feasibility

n_p mole of ith products

LHV_p low heating value of ith products

P plasma power

μ fuel cell efficiency

5.2.2 Steam reforming

Chemical reaction

$C_nH_m + nH_2O \rightarrow nCO + (m/2 + n)H_2$

Reaction enthalpy of steam reforming

$CH_4 + H_2O \rightarrow 3\ H_2 + CO,\ \Delta h = 206.2\ kJ\ mol^{-1}$

$C_2H_4 + 2H_2O \rightarrow 4\ H_2 + CO,\ \Delta h = 210.1\ kJ\ mol^{-1}$

$C_2H_6 + 2H_2O \rightarrow 5\ H_2 + 2CO,\ \Delta h = 347.3\ kJ\ mol^{-1}$

$C_3H_6 + 3H_2O \rightarrow 6\ H_2 + 3\ CO,\ \Delta h = 373.5\ kJ\ mol^{-1}$

$C_3H_8 + 3H_2O \rightarrow 8\ H_2 + 3\ CO,\ \Delta h = 497.7\ kJ\ mol^{-1}$

Steam reforming is highly endothermic

Water gas shift reaction

$CO + H_2O(g) \rightarrow CO_2 + H_2,\ \Delta h = -41.1\ kJ\ mol^{-1}$

- Water shift reaction increases hydrogen in products.
- Due to the exothermic characteristic, slightly high temperature can initiate this reaction.

Steam reforming, as its name, uses steam as an oxidizer to reform hydrocarbons into synthesis gas. In this study, water concentration, power applied on plasma and slightly amount of air, and different flow rates were investigated. In this experiment, discharge gap was 5 mm and the length of discharge was 2 mm. Soot formation on electrode was discussed and influence on the stability of plasma was study. Sight amount of air induced to burn off the soot on electrode and inner wall. Due to water shift reaction, steam reforming generally produces more hydrogen than any other methods. The results of steam and hydrocarbon at different power input, slight air, steam and hydrocarbons at variety of feed-in flow rate, power in input, different steam concentration and changing air flow rate, were study shown in table 4.

H_2/CO ratio analysis

The term of hydrogen / carbon monoxide ratio was used to describe degree of hydrogen riCess in synthesis gas. In this process, H_2/CO ratio is constantly around 3.3, the highest H_2/CO reached at 3.8 in steam reforming. Compared with auto-thermal process, which is around 2 (in later section), steam reforming H_2/CO ratio is 65% higher than auto-thermal process. From the results of Figure 29, high H_2/CO ratio got at lower power density. Red points in Figure 29 represented excessive air in feed-in gas, the present of oxygen consumed part of hydrogen, and this is generally partial oxidation's limitation in hydrogen production.

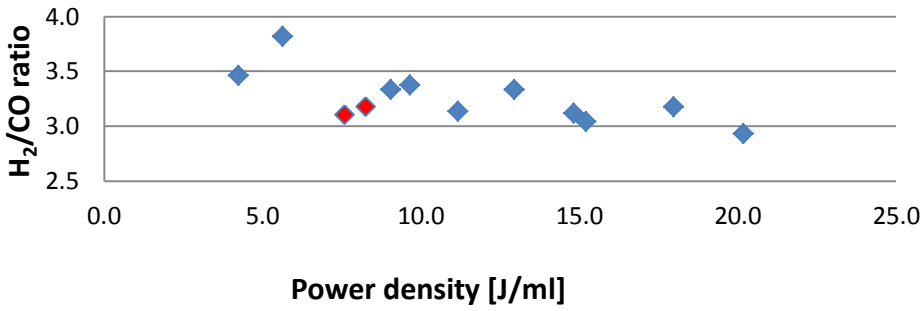

Figure 29. Hydrogen/carbon monoxide ratio I relation with power density

Water gas shift reaction

The water gas shift reaction is a moderately exothermic reversible reaction. Therefore with increasing temperature the reaction rate increases but the conversion of reactants to products becomes less favorable.[37] Due to its exothermic nature, high carbon monoxide conversion is thermodynamically favored at low temperatures. Despite the thermodynamic favorability at low temperatures, the reaction is kinetically favored at high temperatures.[38] The temperature is performed at 600 to 700 K based on catalyst. The elementary steps of mechanism for water gas shift reaction on catalyst in table 5

Table 4. The results of steam reforming

Air flow (sccm)	EPE (sccm)	H_2O/C	Power (W)	H_2	CH_4	CO	CO_2	C_2H_6	C_2H_4	C_3H_6	C_3H_8	C_2H_2	H_2/CO
				2.0%	74.8%	0.0%	4.0%	8.0%	8.0%	2.1%	1.1%	0.0%	
30	64	2.5	17.9	45.80%	29.03%	13.23%	3.20%	2.51%	3.00%	0.36%	0.23%	2.64%	3.5
30	64	2.5	47	54.33%	20.16%	17.33%	3.19%	1.02%	1.85%	0.10%	0.05%	1.97%	3.1
30	64	2.5	63.9	55.39%	18.88%	18.21%	3.39%	0.97%	1.68%	0.10%	0.04%	1.33%	3.0
30	64	3.4	47	50.02%	25.19%	14.99%	3.78%	1.83%	2.42%	0.27%	0.13%	1.36%	3.3
60	64	3.4	47	49.00%	26.48%	15.41%	3.10%	2.01%	2.51%	0.25%	0.13%	1.12%	3.2
90	64	3.4	47	50.68%	24.10%	16.32%	3.40%	1.56%	2.25%	0.20%	0.09%	1.40%	3.1
30	64	1.5	17.9	44.99%	31.18%	11.79%	2.46%	2.61%	3.18%	0.33%	0.18%	3.27%	3.8
30	64	1.5	47	55.08%	19.21%	17.67%	2.68%	0.86%	1.74%	0.11%	0.06%	2.60%	3.1
30	64	1.5	63.9	55.73%	18.53%	19.03%	2.34%	0.84%	1.69%	0.09%	0.04%	1.72%	2.9
-	64	1.5	47	54.91%	20.50%	17.28%	1.76%	1.32%	1.78%	0.14%	0.08%	2.23%	3.2
-	64	2.5	47	53.24%	22.48%	15.98%	2.42%	1.33%	2.06%	0.20%	0.10%	2.20%	3.3
-	64	3.5	47	52.39%	23.33%	15.53%	1.91%	1.60%	2.12%	0.23%	0.14%	2.76%	3.4

Note: H_2O/C is mole ratio, C only count from hydrocarbons.

Table 5. Mechanism for water gas shift reaction on catalyst

Reaction steps	Number
$\mathbf{H_2O + * = H_2O *}$	1
$\mathbf{H_2O + * = OH * + H *}$	2
$\mathbf{2OH * = H_2O * + H *}$	3
$\mathbf{OH * + * = O * + H *}$	4
$\mathbf{2H * = H_2(g) + 2 *}$	5
$\mathbf{CO(g) + * = CO *}$	6
$\mathbf{CO * + O * = CO_2 * + *}$	7
$\mathbf{CO_2 * = CO_2(g) + *}$	8

Note: In the reaction sequence * is surface site and X* is the molecule X absorbed on a site. [39]

Possible pathway for plasma initiate water gas shift reaction at low temperature in steam reforming.

$$e^- + H_2O \rightarrow \dot{H}O + \dot{H} + e^- \quad (1)$$

$$2\dot{H}O \rightarrow H_2O + \dot{H} \quad (2)$$

$$\dot{H}O + e^- \rightarrow \dot{O} + \dot{H} \quad (3)$$

$$2\dot{H} \rightarrow H_2 \quad (4)$$

$$e^- + CO \rightarrow \dot{C}O + e^- \quad (5)$$

$$\dot{C}O + \dot{O} \rightarrow CO_2 \quad (6)$$

As shown in (1)-(6), due to non-thermal plasma characteristic, it can initiate the chemical reaction at low temperature around 100 ºC. And in the steam results, H_2/CO

ratio generally is greater than 3 which means water gas reaction happened in this process.

The hydrogen, carbon monoxide, and unreformed methane were main composition in product stream. The concentration of each component with power density, removed oxide and nitrogen in output stream, showed in figure 30. Hydrogen concentration showed an exponential increasing at power density less than 10 J/ml, yet quick saturated when power reach at 10 J/ml. As same as hydrogen concentration, carbon monoxide concentration mainly came from methane and other higher hydrocarbons dissociation. The concentration of methane, in products, tent to be a constant after power density reached at 12 J/ml as shown in figure 30.

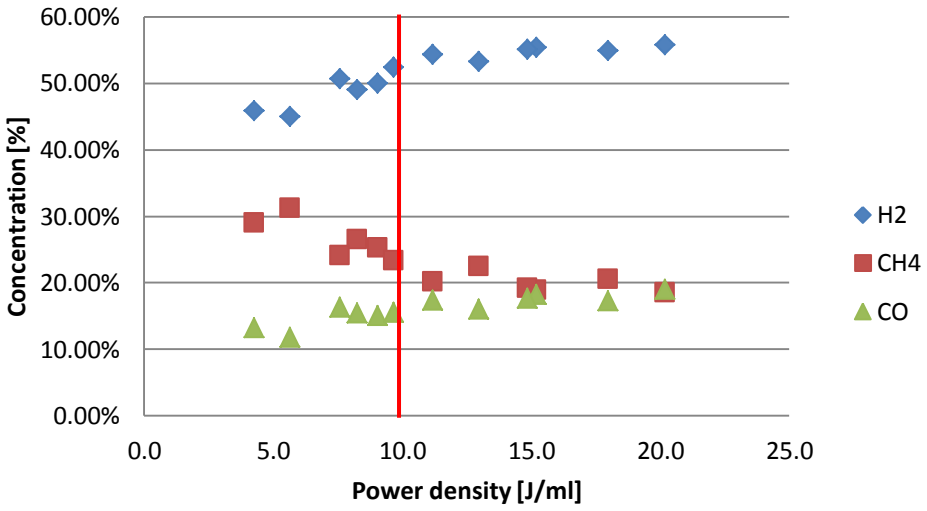

Figure 30. The concentration of hydrogen, carbon monoxide, and unreformed methane after removed oxide and nitrogen in products in relation of power density

Steam reforming with 30 sccm air, 64 sccm, and $H_2O/C=2.5$

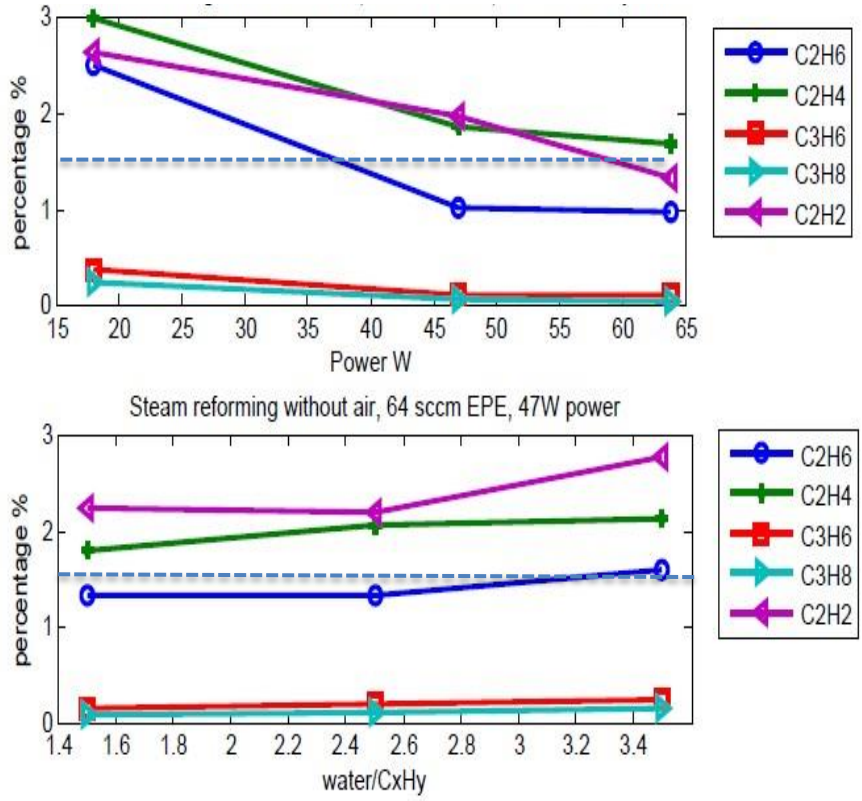

Steam reforming with 64 sccm, 47 W power and H_2O/C ratio

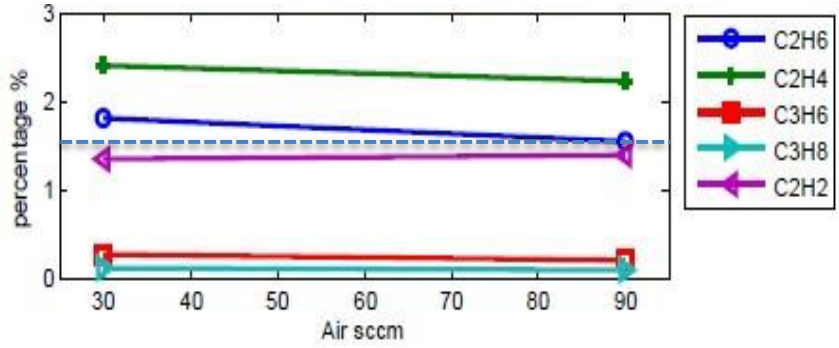

Figure 31. The concentration of ethane, ethylene, acetylene, propane, and propylene after removed oxide and nitrogen in products in relation of power, H_2O/C, and air.

As shown in figure 31, concentration of propane and propylene were decreasing as the power increasing. Lowest concentration reached 0.1% and 0.04%, respectively at a high power 47W and 30 sccm air, 64 sccm EPE gas with 1.5 H_2O/C ratio steam. Higher power also could effectively reduce ethane and ethylene centration in product. Acetylene as a by-product, in steam reforming, had a high concentration 3.27%. In figure 31, both acetylene and ethane had lower concentration because of more air added in. Higher concentration of air in reactants can help to prohibit acetylene formation. High concentration of steam also can confine acetylene formation.

Soot formation

Soot was found at steam reforming process, especially no air participated in. Purely steam and hydrocarbon reforming at 1.5 H_2O/C ratio, severe soot was observed at soot formed on electrode at 64 sccm EPE gas, H_2O/C ratio 1.5, plasma power 47 W, power density18.0 J/ml. As shown in figure 32 a), a thick layer of soot formed on electrode, coordinate with figure 34 a) in which a red hot carbon deposit ring on inner wall. The plasma, in soot formed situation, was not stable and stopped rotating frequently or formed a non-uniform rotating plasma as shown in figure 34 b). A perfect rotating plasma should be uniform and emit white-blue color light in hydrocarbons in in figure 34 c) and can continuous work for 5 hours. Soot formation preferred high power density and less air, small H_2O/C ratio. Air induced in feed-in gas is one way to help clean up soot or prohibit soot formation.

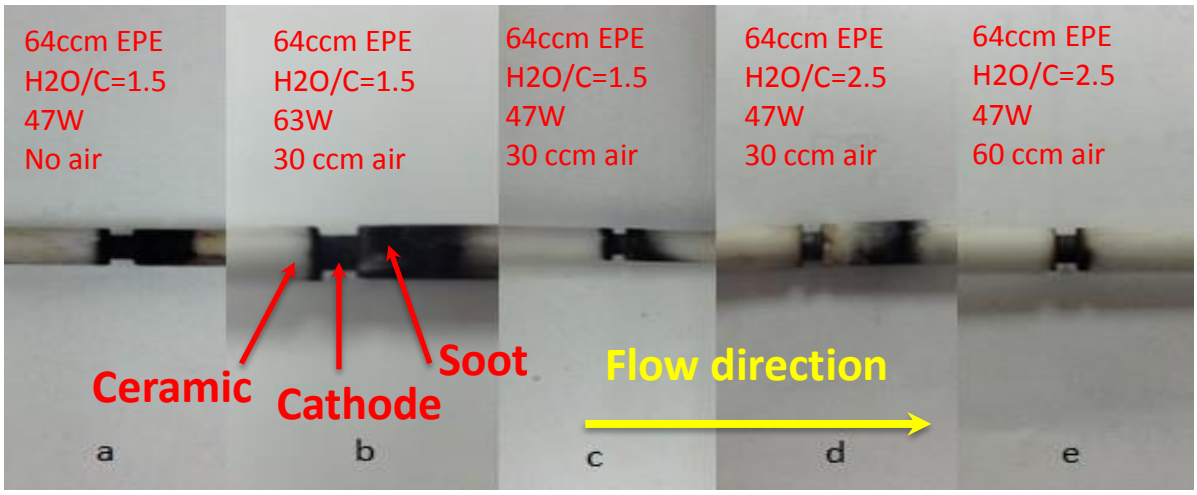

Figure 32. Soot formed on electrode

In figure 32, the soot formation on electrode compared with each figure with constant EPE flow and the variant : power, air flow, and H2O/C ratio.

Conclusion from comparison a&c, b&c, c&d, and d&e.

1 a&c → air reduced soot formation

2 b&c → high power increased soot information

3 c&d → higher H2O/C suppressed soot formation

4 d&e → high H2O/C and more air almost no soot formation

Air & high concentration of steam can suppress soot formation. High power leads to more soot formation.

Plasma stability

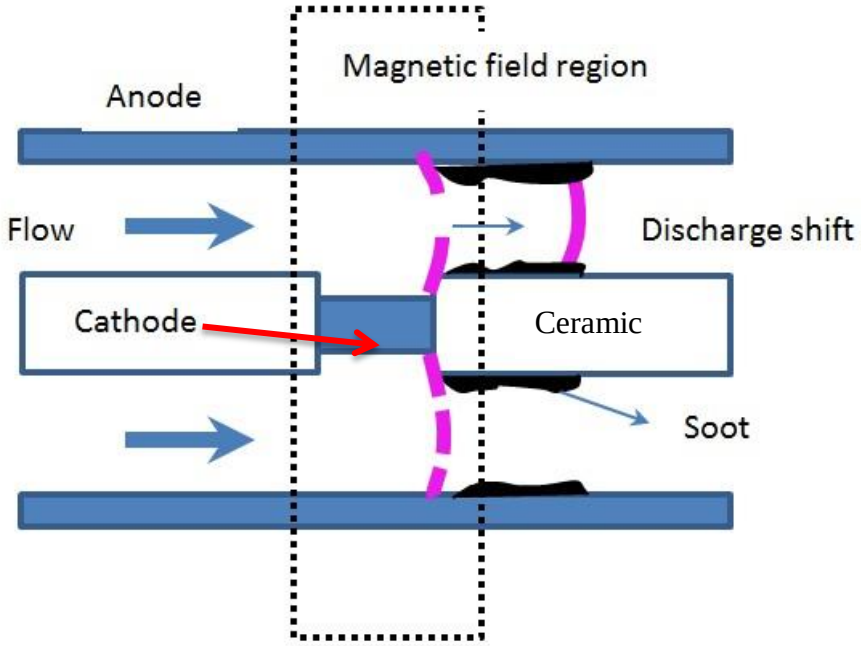

Figure 33. Configuration of discharge shift in soot

Soot is conductive. In addition, plasma always chooses the shortest circuit. So when the soot formed on electrode, the plasma discharge attached to soot by flow blowing the plasma. Then the plasma shifted to soot where out of the high magnetic field and stop rotating as shown in figure 33.

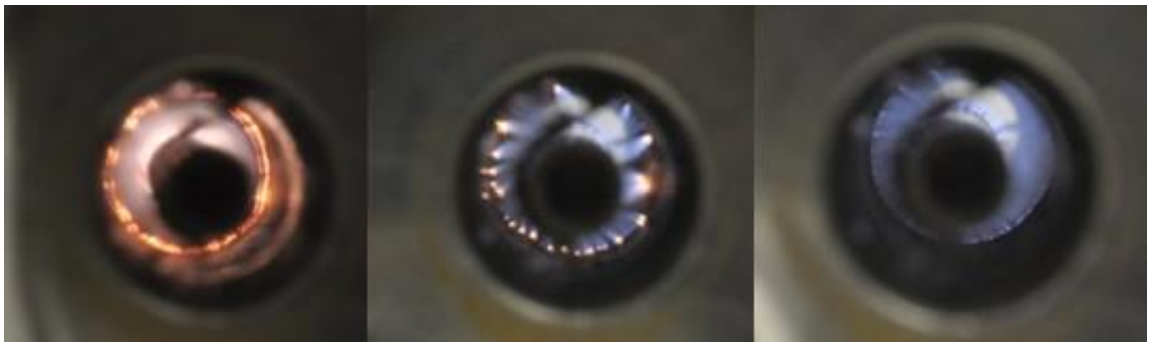

a) b) c)

Figure 34. Examples of soot influence on discharge

a) Severe carbon formation on inner wall and stopping to rotating in 10mins.

b) Non-perfect circle plasma and carbon formation.

c) Ideal rotating plasma can continuously operate greater than 5 hours.

Conclusion of steam reforming

- Steam reforming produces highly hydrogen-rich products
- Steam reforming process is not likely efficiently to clean up higher hydrocarbon gas
- Soot formation will be a problem for this process
- Air can help to clean up soot and suppress soot formation
- Next step: combination air oxide reforming process and steam oxide reforming process will lead to better clean up and slight hydrogen-rich products

5.2.3 Auto-thermal reforming

Steam reforming and partial oxidization process combined by supplying both steam and air to the reformer and adjusting the ratio of oxygen and steam to tune the thermal balance of the reactor. In principle, the reaction enthalpy can be set to zero; this is why the process is called auto-thermal reforming. Compared with steam reforming, less plasma power was spent on heating up to reach the reaction enthalpy. The oxygen helped to convert hydrocarbons and prevent soot and acetylene formation in products. High oxygen concentration (1.08 O_2/C ratio) could convert 99% methane and 100% percent higher hydrocarbons at relatively high power density(7.17 J/ml). However, the selectivity of hydrogen and carbon monoxide got low.

In auto-thermal reforming section, mainly discussion power density and concentration of air influence on reforming hydrocarbons. In the result part, selectivity of hydrogen and carbon monoxide and products concentration were discussed at two O2/C conditions (O2/C=0.72 and O2/C-=1.08) at variety of power densities.

Parameters setup

Small flow rate was set-up for study different O_2/C ratio and power density influence on reformed products, especially the concentration of higher-hydrocarbon (>=C_2H_x) concentration. Also, process efficiency and percentage of plasma power occupied the treated products generated electricity were studied. In other words, how much power consumes in plasma power and the products generate power whether or not can sustain the plasma, and how much electricity can output. Here, we define solid oxide

fuel cell efficiency is 0.5 refer to Hoogers (8). The feasibility θ was calculated as the power on plasma over the products lower heating value(LHV) multiple by fuel cell efficiency.

$$\text{Feasibility } \theta = \frac{Plasma\ Power}{(product\ LHV) * (fuel\ cell\ efficiency)}$$

Steam concentration ranged from 7% to 20% in auto-thermal process in literature (29) (30) (28) (27). Both air and EPE gas were bubbled through warm water, kept 9% steam in total flow rate.

O_2/C_xH_y ratio in partial oxidation process, the electric energy efficiency is optimal at O_2/C=0.6-0.7[1]. The O_2/C ratio are 0.72 and 1.08, respectively.

The plasma power density varied from 0.99 J/ml to 7.71 J/ml.

O_2/C ratio

Basically, O_2/C ratio represent the concentration of oxygen. It influenced on H_2/CO ratio in product, the selectivity of hydrogen, conversion rate of higher hydrocarbons (>=C_2H_x), carbon and acetylene formation.

H_2/CO was used to describe hydrogen richness, the steam reforming reached above 3, and this auto-thermal process H_2/CO ratio lowed to 2. With the increasing concentration of oxygen, H_2/CO ratio tent to decrease. High concentration of oxygen showed that it's more likely to consume more hydrogen than carbon monoxide. In another words, high O_2/C ratio (high concentration of oxygen) limited the selectivity of

hydrogen, 74.8% selectivity of hydrogen at O_2/C ratio 0.72, While 59.3% selectivity of hydrogen at O_2/C ratio 1.08 at 27.9 W power.

High O_2/C ratio (high concentration of oxygen) enhanced the conversion rate of hydrocarbons as shown in table 6. The same power input at 0.81 and 0.72 O_2/C ratio, the conversion rate of O_2/C =0.81, methane, ethane and ethylene increased around 10% and the conversion rate of propane and propylene also slightly increased, because both at a high conversion rate 96.7% and 98.6% respectively at 0.72 O_2/C ratio.

Table 6. Higher-hydrocarbon conversion rate

Air flow	EPE	O_2/C	power	power density	C_2H_6	C_2H_4	C_3H_6	C_3H_8
900	200	0.81	27.9	1.38	73.8%	58.1%	97.5%	99.2%
900	225	0.72	27.9	1.35	67.0%	44.7%	96.7%	98.6%
2000	350	1.08	80	1.86	98.9%	91.3%	100.0%	100.0%
2000	400	0.90	63.9	1.45	51.2%	43.5%	93.4%	98.1%
3000	500	1.08	63.9	1.00	74.1%	57.1%	97.9%	100.0%
3000	750	0.72	17.9	0.26	20.4%	33.7%	88.5%	94.1%
3000	750	0.72	57	0.83	31.8%	35.6%	90.2%	95.6%
3000	750	0.72	80	1.16	52.8%	41.8%	94.1%	97.9%

Carbon and acetylene formation: Due to high concentration of oxygen, no carbon deposit on the electrode and no bright point shown in rotating plasma in figure 35. Overall, acetylene was effectively controlled at less than 1% in high flow rate sets. Higher concentration of oxygen showed a better control of acetylene formation. At the

0.99 J/ml power density set showed a better results of acetylene than power density 1.15J/ml, even lower power density, because of higher O_2/C. The same results in ethane, ethylene, propane and propylene. However, the process efficiency slightly decreased, due to oxygen consumed hydrogen and carbon monoxide.

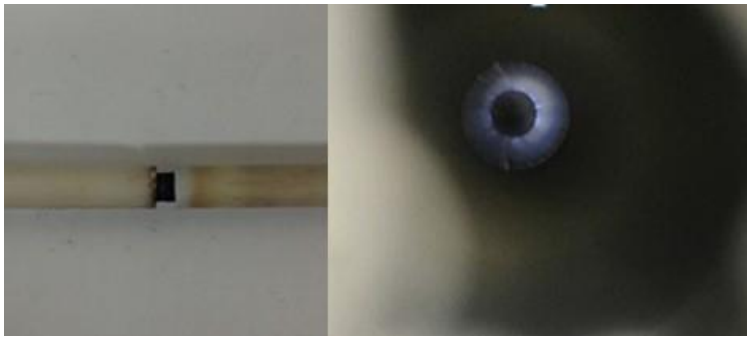

Figure 35. Electrode rotating plasma at O_2/C= 0.72

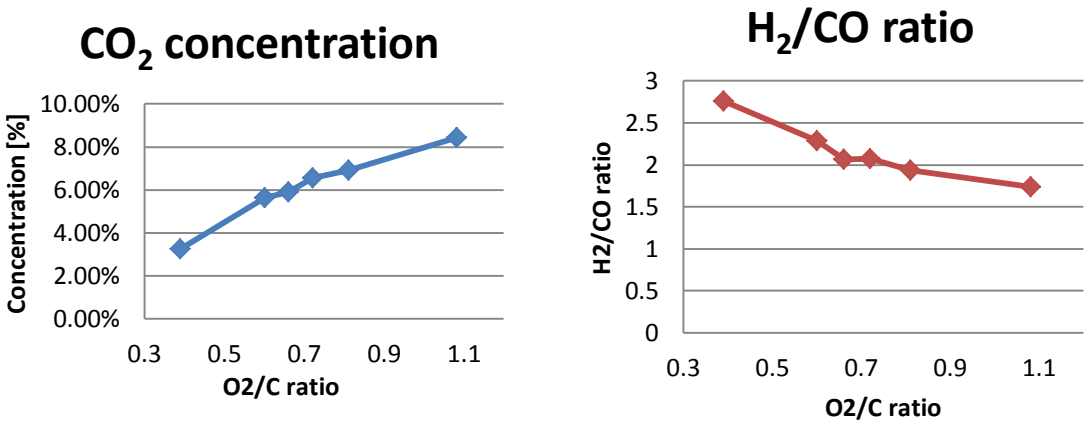

Figure 36. Carbon dioxide concentration and H_2/CO ratio in relation with O_2/C ratio

H_2/CO ratio

In figure 36, while O_2/ C ration varied from 0.4 to 1.1, the H_2/CO ratio decreased from 2.75 to 1.73 and the concentration of carbon dioxide increased 5% in products. This was mainly due to oxygen consumed hydrogen and carbon monoxide. Compared with steam reforming, the minimum H_2/CO ratio was 2.9, with the maximum auto-thermal reforming H_2/CO ratio 2.75, auto-thermal reforming process had a relatively lower hydrogen concentration. However, auto-thermal reforming process can proficiently reduce and confine heavy hydrocarbons in products, which is the goal of this investigation.

The best results of H_2/CO and carbon dioxide concentration were achieved at high flow rate and low power input. In another wards, low power density benefited hydrogen rich and low concentration carbon dioxide products. For example, at 0.83 J/ml power density, 3.21% concentration of carbon dioxide and 2.75 H_2/CO ratio were reached in table 7. Whereas, the concentration of heavy hydrocarbon were high, ethane and ethylene concentration were above 3%, which is due to low conversion at low power density. In order to achieve lower higher-hydrocarbon ($>=C_2H_x$) concentration, the H_2/CO ratio would have to be around 2 or lower as a trade-off between higher-hydrocarbon ($>=C_2H_x$) and H_2/CO ratio.

Power density

Power density is the product power over flow rate. It's more accurate to describe what the relation between different power and different flow rate happen on discharge.

Table 7. Auto-thermal reforming result of O_2/C =0.72

Total flow rate sccm	Air flow sccm	EPE sccm	O_2/C	Power W	power density J/ml	H_2	CH_4	CO	CO_2	C_2H_6	C_2H_4	C_3H_6	C_3H_8	C_2H_2	Process efficiency	plasma power/ electricity generated
4125	3000	745	0.72	57	0.83	29.65%	45.87%	12.41%	3.21%	3.77%	3.56%	0.54%	0.24%	0.75%	87.20%	25.30%
4125	3000	745	0.72	80	1.16	34.89%	39.45%	15.81%	3.52%	2.30%	2.83%	0.29%	0.10%	0.82%	84.30%	35.20%
1237	900	225	0.72	27.9	1.35	41.94%	26.94%	20.61%	5.44%	1.47%	2.47%	0.15%	0.06%	0.91%	74.70%	45.10%
412.5	300	75	0.72	18.9	2.75	46.21%	22.22%	21.69%	5.97%	0.99%	1.96%	0.00%	0.00%	0.96%	69.50%	83.90%
412.5	300	75	0.72	27.9	4.06	51.43%	14.90%	24.82%	6.57%	0.34%	1.15%	0.00%	0.00%	0.79%	59.60%	126.80%
412.5	300	75	0.72	46	6.69	57.95%	6.80%	27.19%	6.93%	0.06%	0.40%	0.00%	0.00%	0.67%	43.10%	232.20%

Note: H_2O/C is mole ratio, C only count from hydrocarbons.

9% steam in the total flow rate.

Power density=Power of plasma /total flow rate.

Plasma power/ electricity generated (feasibility) = $\frac{\text{Plasma Power}}{(\text{product LHV}) * (\text{fuel cell efficiency})} * 100\%.$

O_2/C ratio =0.72

Trend study

300 sccm air and 75 sccm EPE gas set: Lower O_2/C ratio 0.72 was tested. Due to low concentration of propane and propylene in reactant, 1.1% and 2.1% respectively, the conversion efficiency kept 100% for both at different power input. However, the conversion rate of methane, ethane, and ethylene were 38%, 74% and 48.6%, respectively at 18.9 W power input in table 8. The concentration of hydrocarbons of the O_2/C =0.72 at 18.9 W power input set were high, the concentration of ethylene reached 1.96%, ethane was 0.99% and the acetylene had 0.96%. Although the process efficiency reached as high as 69.5% and the feasibility, firstly below 100%, reached 83.9% in table 8, the products is unlikely for electricity generation because of high concentration of higher-hydrocarbons (>=C_2H_x).

As increasing the power input, conversion of each component was increased and the by-product acetylene was prohibited at low concentration in product. Although, the process efficiency of O_2/C = 0.72 got higher and feasibility reduce to a lower level, O_2/C = 0.72 set had lower conversion rate and high acetylene produced at low power density.

In table 8, with 27.9 W power input, the concentration rate of ethane, acetylene and ethylene were 0.36% , 0.79% and 1.15%, respectively, and no trace of propane and propylene. Except ethylene was higher than 1%, the centration of others were effectively controlled, while the process efficiency was 59.2% and feasibility was 126.8% which was not economic. At 46.W power input, all the higher-hydrocarbon (>=C_2H_x) were

effectively controlled. The concentration of ethane, acetylene and ethylene were 0.06%, 0.67% and 0.40%, respectively, and no trace of propane and propylene. However, the process efficiency and feasibility got worse, 43.1% and 232.1% respectively.

Table 8. Hydrocarbon conversion rate at O_2/C=0.72

Air flow	EPE	O_2/C	power	power density	conversion rate CH_4	C_2H_6	C_2H_4	C_3H_6	C_3H_8	Selectivity H_2
300	75	0.72	18.9	2.75	38%	74.0%	48.6%	100%	100%	75.1%
300	75	0.72	27.9	4.06	51%	89.4%	64.5%	100%	100%	74.9%
300	75	0.72	46.0	6.69	76%	98.0%	86.6%	100%	100%	63.4%
3000	750	0.72	57	0.83	11.2%	31.8%	35.6%	90.2%	95.6%	-
3000	750	0.72	80	1.16	13.2%	52.8%	41.8%	94.1%	97.9%	-

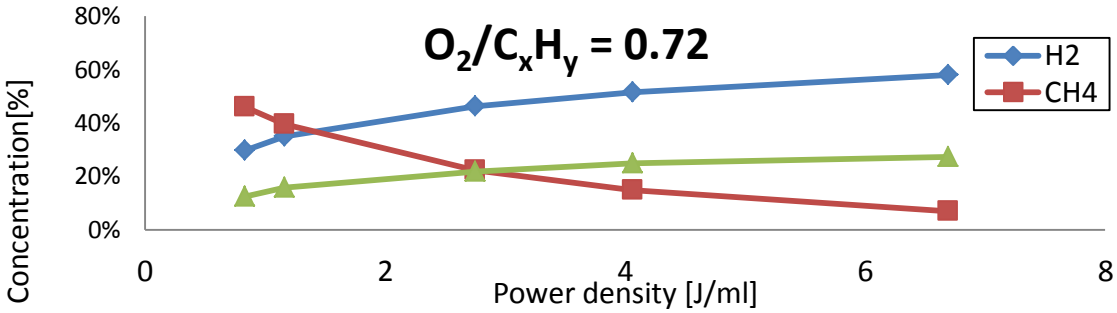

Figure 37. Concentration of hydrogen, methane and carbon monoxide over power density at O_2/C = 0.72

Optimization

Low flow rate studied the posssibility of cleaning up higher hydrocarbons (>=C_2H_x) or keeping at low concentration less 1%. The relation between concentration of oxygen as oxidizer and the concentration of higher hydrocarbons in product was studied. Higher oxygen concentratoin help convert higher hydrocarbons and prevent large amount of acetylene formation. Whereas, higher concentraiton came with a drawback that limitation of hydrogen and carbon monoxide via burning off both of them. Thereby, the process efficiency was lower and feasibility got higher. The higher power input, the lower process efficiency and more unlikely self-electricty-sustainable. Another reason is that low flow rate carried with low heating value power (LHVP). For example, 50 sccm EPE gas came with 30.6 W(LHVP). After the plsma treatment, the product gases caried with slightly less than 30.6 W (LHVP). Meanwhile, the plasma power was 46 W were relatively higher than products LHVP, that's why the process efficiency was low and feasibility was too high. However, all of concentraotn higher hydrocarbons (>=C_2H_x) were effectively controlled at less than 1% in product stream. Thus, it's possible that ran high flow rate at a relatively low power density, while higher hydrocarbons (>=C_2H_x) were controlled at low concentration.

In the optimized result, mainly study the concentration of products, process efficiency and feasibility. The mainly products, hydrogen, carbon monoxide and unreformed methane were plotted in relation with power density. As shown in figure 37, at low power density around 40% methane in product and the conversion rate was low

between 10% to 15% as shown table 8. Also carbon monoxide and hydrogen concentration were low. With the power density increasing, higher conversion rate, and more carbon monoxide and hydrogen achieved.

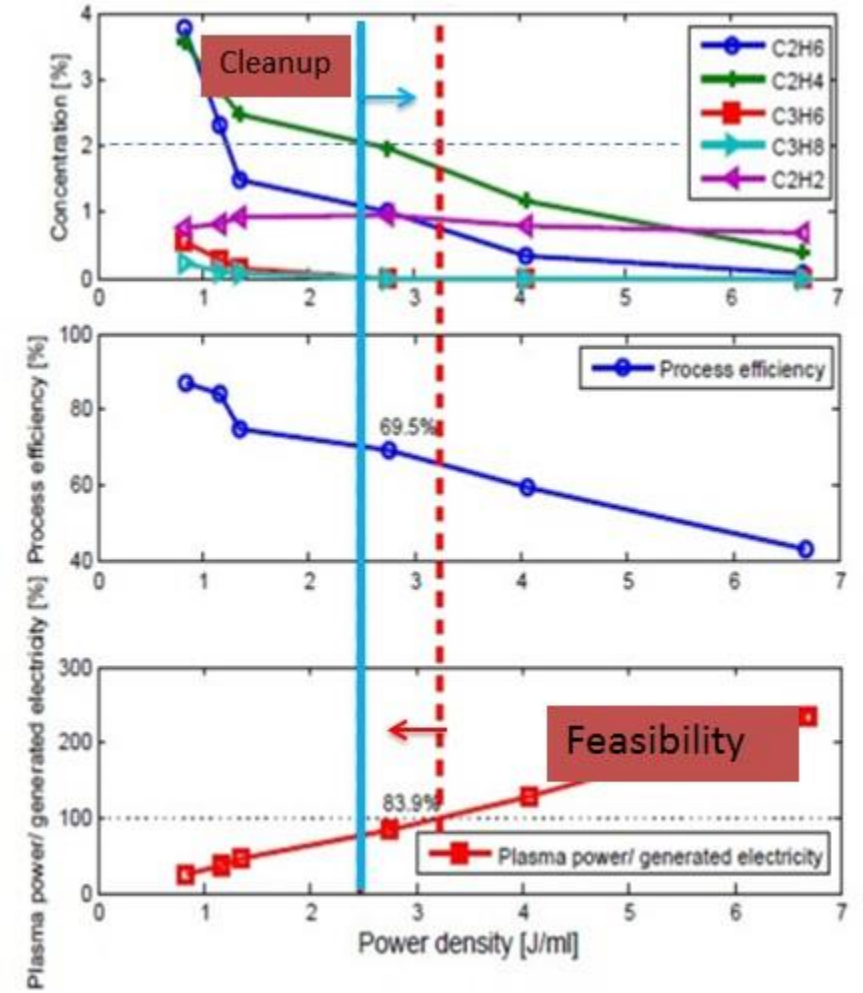

Figure 38. Concentration, and process efficiency and feasibilty over power density at $O_2/C = 0.72$ and 9% steam

The cleanup results and feasibility are two criteria in optimal process. Cleanup and feasibility are trade-off. The high clean up results(low concentration for each higher hydrocarbons) were achieved at less feasible power efficiency. While high feasible power efficiency, clean up results didn't meet the goal as shown in figure 38. Clean up criteria for O2/C=0.72 set is both ethane and ethylene <2%, C3H8<0.42%, C3H6<0.22%, and C2H2<1%. The feasibility is less than 100%. At low power density at around 1J/ml, ethane and ethylene were both greater than 3% and also propene and propane didn't meet the goal. Until the power density increased to 2.5 J/ml, concentration of propene and propane also were 0% and ethylene and ethane lower than 2%. The acetylene didn't show any trend: decreeing with power density increasing. But it kept lower than 1% in this study. The feasibility reached 100% at 3.2 J/ml. if process at greater than 3.2 J/ml power density, this process would not self-sustainable. From these two criteria, operate power density region of O2/C=0.72 set was 2.5 J/ml to 3.2J/ml. In order to get best power efficiency, while the cleanup result is acceptable, 2.5 J/ml will be an ideal operation power density for O2/C=0.72 set.

O_2/C ratio=1.08

Trend study at low flow rate

300 sccm air and 50 sccm EPE gas (O_2/C=1.08) : variation in higher-hydrocarbon conversion with respect to changing power in plasma is shown in table 9. Propane and propylene achieved 100% conversion efficiency, mainly because low concentration in reactant 1.1% and 2.1% respectively, also power density was high

enough. Part of ethane was converted into ethylene by losing two hydrogen atoms. Thereby, the conversion of ethylene was slightly lower than the conversion of ethane, as shown in table 9, except they both reached 100% conversion efficiency. Higher powers show better conversion towards ethylene and ethane, and 100% conversion efficiency for each, while lowering the selectivity of hydrogen. This is the effect of increase in electron density leading to generation of more hydrogen ions and oxygen ions directly formed water in product. The selectivity of hydrogen of different power input sets were all less than 50%, in that it is also due to high O_2/C ratio1.08. Excessive oxygen consumed hydrogen and carbon monoxide, also lead a high selectivity to carbon dioxide as high as 15% to 17% in product as shown in table 9. The concentration of hydrogen increased with higher power, which was resulted from dissociation of methane. The methane conversion rate reached 98%, while other hydrocarbon conversion efficiency was 100% at a relatively high power 47W and power density 7.17 J/ml.

Table 9. Hydrocarbon conversion rate O_2/C=1.08

Air flow sccm	EPE sccm	O_2/C	Power W	power density J/ml	C_2H_6	C_2H_4	C_3H_6	C_3H_8	Selectivity H_2
300	50	1.08	18.9	2.95	90.0%	79.1%	100.0%	100.0%	<50%
300	50	1.08	27.9	4.35	97.6%	94.2%	100.0%	100.0%	<50%
300	50	1.08	37	5.77	100.0%	97.3%	100.0%	100.0%	<50%
300	50	1.08	46	7.17	100.0%	100.0%	100.0%	100.0%	<50%
3000	500	1.08	63.9	1.00	74.1%	57.1%	97.9%	100.0%	-
2000	350	1.08	80	1.86	98.9%	91.3%	100.0%	100.0%	-

However, process efficiency and feasibility were not economical in table 10. The best process efficiency was 43.9%. It appears that most plasma and fuel energy were lost as heat lose. Besides, feasibility was 173.8%, which means the electricity generated by clean-up fuel even cannot sustain the plasma power. With higher plasma power input, the lower process efficiency and tend to be un-self-sustainable, although it proved higher conversion of hydrocarbons. At 7.17 J/ml density power, the process efficiency lowed to 27.1 and the feasibility was reach 442.9%.

Optimization

Low flow rate studied the posssibility of cleaning up higher hydrocarbons (>=C_2H_x) or keeping at low concentration less 1%. The relation between concentration of oxygen as oxidizer and the concentration of higher hydrocarbons in product was studied. Also low flow rate ran at high power densities ranged from 2.75 J/ml to 7.17 J/ml at O2/C ratio= 1.08. The higher hydrocarbons (>=C_2H_x) comveraation rate was reached more than 79% at 2.75 J/ml and another one: all hydrocarbons 100% converted except methane 98% converstion rate at 7.17 J/ml. Besides all of concentraotn higher hydrocarbons (>=C_2H_x) were effectively controlled at less than 1% in product stream. Thus, it's possible that ran high flow rate at a relatively low power density, while higher hydrocarbons (>=C_2H_x) were controlled at low concentration.

Table 10. Auto-thermal reforming result of O_2/C =1.08

Total flow rate sccm	Air flow sccm	EPE sccm	O_2/C	Power W	power density J/ml	H_2	CH_4	CO	CO_2	C_2H_6	C_2H_4	C_3H_6	C_3H_8	C_2H_2	Process efficiency	plasma power/ electricity generated
3850	3000	500	1.08	63.9	0.99	42.27%	21.68%	24.34%	8.44%	1.01%	1.67%	0.08%	0.00%	0.50%	74.40%	46.40%
2585	2000	335	1.08	80	1.86	42.11%	25.62%	24.01%	7.38%	0.04%	0.32%	0.00%	0.00%	0.53%	64.90%	83.70%
385	300	50	1.08	27.9	4.35	51.49%	4.28%	26.49%	17.31%	0.08%	0.19%	0.00%	0.00%	0.16%	35.80%	266.50%
385	300	50	1.08	37	5.77	53.10%	4.28%	25.92%	16.61%	0.00%	0.09%	0.00%	0.00%	0.00%	30.90%	354.30%
385	300	50	1.08	46	7.17	56.19%	0.66%	26.55%	16.59%	0.00%	0.00%	0.00%	0.00%	0.00%	27.10%	442.90%

Note: H_2O/C is mole ratio, C only count from hydrocarbons.

9% steam in the total flow rate.

Power density=Power of plasma /total flow rate.

Plasma power/ electricity generated (feasibility) = $\frac{\text{Plasma Power}}{(\text{product LHV}) * (\text{fuel cell efficiency})} * 100\%.$

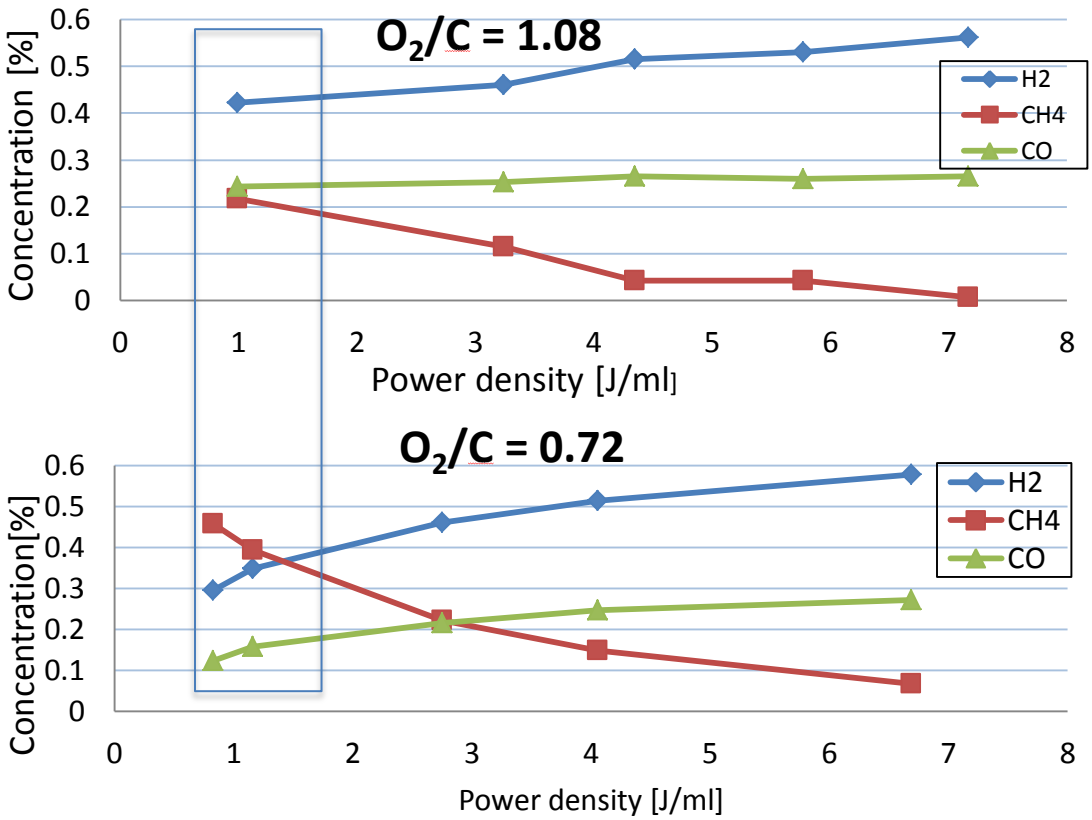

Figure 39. Concentration of hydrogen, methane and carbon monoxide over power density at $O_2/C = 1.08$, compared with $O_2/C = 0.72$

In figure 39, Compared with the O2/C=0.72 set, the O2/C=1.08 set had a lower concentration of methane and also higher concentration of hydrogen and carbon monoxide. For example, O2/C=0.72 set had 34.89% hydrogen, 39.45% unreformed methane and 15.81% carbon monoxide in product at 1.16 J/ml power density in table 8. The conversion rate of methane was 13.2% in table 7. The O2/C=1.08 had 42.27% hydrogen, 21.68% unreformed methane and 24.34% carbon monoxide in product at 0.99

J/ml power density in table 10. That means O2/C=1.08 improved the conversion of hydrogen carbons at lower power density, another words, O2/C=1.08 had a better clean up results and also low energy cost.

Clean up criteria for O2/C=1.08 set is both ethane and ethylene <1.6%, C3H8<0.42%, C3H6<0.22%, and C2H2<1%. The feasibility is less than 100. At low power density at around 1 J/ml, ethane and ethylene were both qualified and also propene and propane meet the goal% in figure 40. With the power density increasing to 2.2 J/ml, concentration of acetylene kept around 0.5% and tend to decreasing with power density increasing. The concentration of propene and propane also were 0% and ethylene and ethane lower than 0.4%. With higher power density input, the concentration of them can be lower than 0.1% at around 7 J/ml power density, at the expense of feasibility. The feasibility reached 100% at 2.2 J/ml. if process at greater than 2.2 J/ml power density, this process would not self-sustainable. From these two criteria, operate power density region of O2/C=1.08 set was 0.99 J/ml to 2.2J/ml. In order to get best power efficiency, while the cleanup result is acceptable, 0.99 J/ml will be an ideal operation power density for O2/C=1.08 set. Compared with O2/C= 0.72 set lower power density operation region was achieved and higher process efficiency and low feasibility as shown in figure 40.

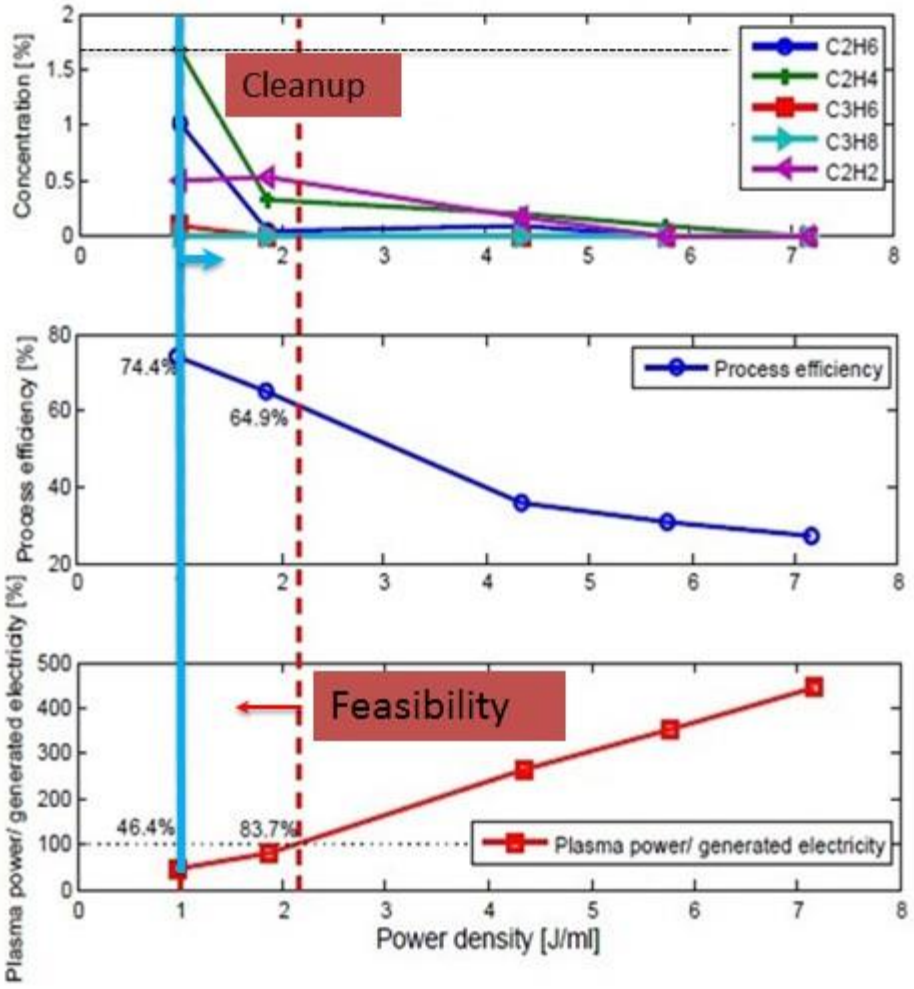

Figure 40. Concnetration, and process efficiency over power density O_2/C= 1.08 and 9% steam

Process efficiency and feasibility

As an ideal result, process efficiency, the higher, the better and feasibility the lower, the better. Process efficiency decreased with power density increasing. Also, O_2/C ratio played an important role in process efficiency. High O_2/C could burn part of hydrogen and carbon monoxide and reduce the process efficiency. In order to self-sustainable, feasibility should be less than 100% and the less power spends on plasma, the more electricity can get from fuel cell.

All process efficiency was higher than 70%, the highest reached 91.6% and the feasibility ranged from 8.2% to 79.5%. However, goal of this process, reduces the concentration of higher hydrocarbons (>=C_2H_x) as small concentration as possible, while maintain a high process efficiency and a low feasibility. For example, as shown in figure 40, with 0.99 J/ml power density and 1.08 O_2/C ratio set achieved 74.4% process efficiency and 46.4% feasibility. At same time, the concentration of ethane, ethylene, propane, propylene, and acetylene were 1.01%, 1.67%, 0.08%, 0.00%, and 0.50%, respectively. The concentration of ethylene was slight higher. Another result showed that at1.84 J/ml power density and 1.08 O_2/C ratio achieved 69.2% process efficiency and 78.5% feasibility. While the concentration of ethane, ethylene, propane, propylene, and acetylene were 0.04%, 0.32%, 0.00%, 0.00%, and 0.53%, respectively. The total concentration of higher hydrocarbons (>=C_2H_x) was less than 1%. The potential set was at1.16 J/ml power density and 0.72 O_2/C ratio achieved 84.3% process efficiency and 35.2% feasibility, while the concentration of ethane, ethylene, propane, propylene, and

acetylene were 2.30%,2.83%, 0.29%,0.10%, and 0.82%. Due to air as the oxidizer, there was 57.5% to 61.5% nitrogen in total flow rate. Nitrogen in plasma took part of energy and then vibrational and electronic excited which also did penning process initiate hydrocarbon radical. However, part of energy lost by vibration relaxation, electronic relaxation and heat loss. Use pure oxygen instead of air would get a promising result, because more than 2 times power density would greatly increase the higher hydrocarbons (>=C_2H_x) conversion rate.

6. CONCLUSION AND FUTURE WORK

6.1 Research goal accomplished in this work

- Built experiment plasma prototype with control at hydrocarbon gas, nitrogen, steam, air, plasma power, preheat up, and magnetic field
- Spectrometer detected ammonia generated from steam and nitrogen
- Calibrated Gas chromatography and GC-MS gas analysis
- Plasma device tested and optimized: continuously work greater than 5 hours.
- Calculated the concentration, conversion rate, process efficiency and feasibility
- Optimization for hydrocarbon cleanup process

6.2 Ammonia synthesis

Small compact glow discharge was applied to investigate ammonia synthesis from steam and nitrogen. Ammonia was successfully detected via UV-VIS absorbance and the highest pH value of solution reached 8.2. Ammonia generation in future work need focus on quantifying the ammonia production and increasing the selectivity of ammonia.

6.3 EPE cleanup

6.3.1 Steam reforming

Steam reforming process benefit hydrogen rich production. The minimum H_2/CO was 2.9 in this study. Due to steam reforming is highly endothermic, large amount of energy was spent on heat up gas to initiate this process. Thus, the energy consumption is high; the energy density ranged from 5 J/ml to 20 J/ml, while several times more than auto-thermal process. From the results, steam reforming didn't effectively prevent acetylene formation, meanwhile, it's more likely benefit acetylene formation. The highest concentration of acetylene 3.27% was observed. Higher hydrocarbons (>=C_2H_x) wasn't cleanup as well, ethane and ethylene was higher than 1% in products. Soot formation is another problem in steam reforming. Severe soot formed at 1.5 H_2O/C ratio. Less soot requested high H_2O/C >3 which wasn't energy efficient.

6.3.2 Auto-thermal process

Auto-thermal process: combine steam reforming and partial oxidation reforming to tune the thermal balance of the reaction. Compared with steam reforming, less plasma power was spent on heating up to reach the reaction enthalpy. The mainly drawback is that consume hydrogen and carbon monoxide and low H_2/CO ratio, generally less than 2. The effective power density was varied 1J/ml to 2 J/ml. The low concentration of higher hydrocarbons (>=C_2H_x), considered successful results, were achieve.

O_2/C ratio: O_2/C ratios ranged from 0.72 to 1.08 were tested. The trend of air addition is that increasing the conversation rate of all hydrocarbons. However, high

concentration of oxygen showed that it's more likely to consume more hydrogen than carbon monoxide. In another words, high O_2/C ratio (high concentration of oxygen) limited the selectivity of hydrogen, 74.8% selectivity of hydrogen at O_2/C ratio 0.72, While 59.3% selectivity of hydrogen at O_2/C ratio 1.08 at 4J/ml power density. In addition, H_2/CO ratio was less than 2. After all, relative higher O_2/C ratio achieve an excellent clean up results, for example, when O_2/C ratio equal to 1.08 at 1.98 J/ml power density achieve great than 90% conversion rate in higher hydrocarbon(=>C_2H_x). Also, higher O_2/C ratio reached better conversion results at lower power density.

Power density: as shown in trend studied and optimization part, higher power density always can increasing the conversion rate. However, it's directly related to process efficiency and feasibility. Higher power density will not be efficient. In this study the best power density operation zone was optimized in: when O_2/C ratio = 0.72, the most energy efficient region is 2.5J/ml to 3.2 J/ml. While O_2/C ratio = 1.08, the most energy efficient region is 1J/ml to 2.2 J/ml.

Optimized results: 1.84 J/ml power density and 1.08 O_2/C ratio condition achieved 69.2% process efficiency and 78.5% feasibility. At the sometime, the concentration of ethane, ethylene, propane, propylene, and acetylene were 0.04%, 0.32%, no trace, no trace, and 0.53%, respectively. The total concentration of higher hydrocarbons (>=C_2H_x) was less than 1%. There no carbon deposit was observed on electrode and inner wall. Overall, acetylene was effectively controlled at less 1%.

6.3.3 Future work

Although this process efficiency wasn't high enough and the feasibility was too high to be economical, it's showed the potential to get better. In auto-thermal process, Due to air use as oxidizer, 60% of nitrogen & energy sink in total flow rate. if using pure oxygen to instead of air, it would increase both the conversion rate and process efficiency and maybe economic.

The acetylene control would be a challenge. Choosing lower energy type plasma like dielectric barrier discharge or DC pulse power supply would reduce the formation of acetylene.

REFERENCES

1. Fridman, A., *Plasma chemistry*. Cambridge University Press, New York, 2008.

2. Trachoo, N. and J.F. Frank, *Effectiveness of chemical sanitizers against Campylobacter jejuni-containing biofilms.* Journal of Food, 2002. **65**(7): p. 1117-1121.

3. Sharma, M.N. and E.B. White, *Method of sanitizing a volume of water in conjunction with chlorine*. Patents US4119535 A, Bensenville, IL, 1978.

4. Iitsuka, Y., et al., *Ammonia production from solid urea using nonthermal plasma*. Industry Applications, IEEE Transactions on, 2012. **48**(3): p. 872-877.

5. NaturalGas.org. *Overview of natural gas*. *Resources* 2004, cited 2014; Available from: *Http://naturalgas.org/overview/resources/*

6. NaturalGas.org. *Overview of natural gas*. *Background* 2004, cited 2014; Available from: *Http://naturalgas.org/overview/background/*

7. York, A.P., T. Xiao, and M.L. Green, *Brief overview of the partial oxidation of methane to synthesis gas.* Topics in Catalysis, 2003. **22**(3-4): p. 345-358.

8. Hoogers, G., *Fuel cell technology handbook.* CRC Press, New York, 2002.

9. Shekhawat II, D., J.J. Spivey, and D.A. Berry, *Fuel cells: technologies for fuel processing: technologies for fuel processing*. Elsevier, Oxford, UK, 2011.

10. LM Zhou, B Xue, U Kogelschatz, B Eliasson., *Nonequilibrium plasma reforming of greenhouse gases to synthesis gas.* Energy & Fuels, 1998. **12**(6): p. 1191-1199.

11. Pârvulescu, V.I., M. Magureanu, and P. Lukes, *Plasma chemistry and catalysis in gases and liquids*. John Wiley & Sons, Weiheim, Germany, 2012.

12. Raizer, Y.P., V.I. Kisin, and J.E. Allen, *Gas discharge physics*. Springer, New York 1991.

13. Thunderbolts.info. *Currents, Filaments and Pinches*. The Voltage-Current Curve 2009, cited 2014; Available from: *Http://www.thunderbolts.info/eg_draft/eg_chapter_6.htm*

14. Glow-discharge.com, *Discharge Regimes.* 2014, cited 2014; Available from: *Http://www.glow-discharge.com/?physical_background:glow_discharges:discharge_regimes*

15. Wikipedia. *Electric glow discharge schematic*. 2009, cited 2014; Available from: *Http://en.wikipedia.org/wiki/file:electric_glow_discharge_schematic.png*

16. Staack, D., et al., *Characterization of a dc atmospheric pressure normal glow discharge.* Plasma Sources Science and Technology, 2005. **14**(4): p. 700.

17. Staack, D., et al., *Spectroscopic studies and rotational and vibrational temperature measurements of atmospheric pressure normal glow plasma discharges in air.* Plasma Sources Science and Technology, 2006. **15**(4): p. 818.

18. Günther, D. and B. Hattendorf, *Solid sample analysis using laser ablation inductively coupled plasma mass spectrometry.* TrAC Trends in Analytical Chemistry, 2005. **24**(3): p. 255-265.

19. Kogelschatz, U., *Dielectric-barrier discharges: their history, discharge physics, and industrial applications.* Plasma Chemistry and Plasma Processing, 2003. **23**(1): p. 1-46.

20. Fridman, A., et al., *Gliding arc gas discharge.* Progress in Energy and Combustion Science, 1998. **25**(2): p. 211-231.

21. Cheng, D.-g., et al., *Carbon dioxide reforming of methane over Ni/Al_2O_3 treated with glow discharge plasma.* Catalysis Today, 2006. **115**(1): p. 205-210.

22. Gallagher, M.J., et al., *On-board plasma-assisted conversion of heavy hydrocarbons into synthesis gas.* Fuel, 2010. **89**(6): p. 1187-1192.

23. Hammer, T., T. Kappes, and W. Schiene. *Conversion of methane and other greenhouse gases via plasmas or microwave heating-19 plasma catalytic hybrid reforming of methane*. in *ACS symposium series*. American Chemical Society, Washington, DC, 2003.

24. Wang, Y.-F., et al., *Methane steam reforming for producing hydrogen in an atmospheric-pressure microwave plasma reactor.* International Journal of Hydrogen Energy, 2010. **35**(1): p. 135-140.

25. Pietruszka, B. and M. Heintze, *Methane conversion at low temperature: the combined application of catalysis and non-equilibrium plasma.* Catalysis Today, 2004. **90**(1): p. 151-158.

26. Pornmai, K., et al., *Synthesis gas production from co2-containing natural gas by combined steam reforming and partial oxidation in an ac gliding arc discharge*. Plasma Chemistry and Plasma Processing, 2012. **32**(4): p. 723-742.

27. Cormier, J.M. and I. Rusu, *Syngas production via methane steam reforming with oxygen: plasma reactors versus chemical reactors.* Journal of Physics D: Applied Physics, 2001. **34**(18): p. 2798.

28. Zhou, Z., et al., *Hydrogen production by reforming methane in a corona inducing dielectric barrier discharge and catalyst hybrid reactor.* Chinese Science Bulletin, 2011. **56**(20): p. 2162-2166.

29. Piavis, W. and S. Turn, *An experimental investigation of reverse vortex flow plasma reforming of methane.* International Journal of Hydrogen Energy, 2012. **37**(22): p. 17078-17092.

30. X Guo, Y Sun, Y Yu, X Zhu, C Liu, *Carbon formation and steam reforming of methane on silica supported nickel catalysts.* Catalysis Communications, 2012. **19**: p. 61-65.

31. Nozaki, T., et al., *Dissociation of vibrationally excited methane on Ni catalyst: Part 1. Application to methane steam reforming.* Catalysis Today, 2004. **89**(1): p. 57-65.

32. Ghorbanzadeh, A., R. Lotfalipour, and S. Rezaei, *Carbon dioxide reforming of methane at near room temperature in low energy pulsed plasma.* International Journal of Hydrogen Energy, 2009. **34**(1): p. 293-298.

33. Magnetics, K.J. *Magfield.asp?pname=rx4c2,* 2014, cited 2014; Available from: *Http://www.kjmagnetics.com/magfield.asp?pName=RX4C2*

34. EXTORR. *Residual gas analyzer*. 2006, cited 2014; Available from: *Http://www.extorr.com/products.htm*

35. SRI Instruments, *Model 8610C gas chromatograph manual*. 2014, cited 2014; Available from: *Http://www.srigc.com/MG3.pdf*

36. Walsh, A. and P. Warsop, *The ultra-violet absorption spectrum of ammonia.* Transactions of the Faraday Society, 1961. **57**: p. 345-358.

37. Ratnasamy, C. and J.P. Wagner, *Water gas shift catalysis.* Catalysis Reviews, 2009. **51**(3): p. 325-440.

38. Callaghan, C.A., *Kinetics and catalysis of the water-gas-shift reaction: A microkinetic and graph theoretic approach*. Worcester Polytechnic Institute, Worcester, MA, 2006.

39. Ovesen, C., et al., *A kinetic model of the water gas shift reaction.* Journal of Catalysis, 1992. **134**(2): p. 445-468.

APPENDIX

Gas Chromatography Operation Setup:

The cylinder head pressure 45 psi, carrier gas pressure 21 psi.

Gas Chromatography Program steps:

Temperature setup:

Initial temperautre	hold
40 C	4 mins
ramp	finial tmeperature
20 C/min	160 C
hold	total time
15 mins	25 mins

Event:

Time (min)	Event
0	-
0.05	G on (valve rotating)
6	G off (valve rotating)

Species eluting time:

Species	Time(min)
Hydrogen	1.2
Oxygen	2
Nitrogen	2.3
Carbon monoxide	3.5
Methane	4.05
Ethane	7.37
Carbon dioxide	8.46
Ethylene	8.9
Propene	10.6
Acetylene	11.1
Propane	13.25

Gas Chromatography (GC) Calibration data: Hydrocarbon gas (EPE), CO, Acetylene, and Hydrogen.

Spices	Area	Percentage	A/P calibration factor
hydrogen	162.5	2.0%	8125
methane	9689.3	74.8%	12954
ethane	3949.3	8.0%	49366
CO2	1078.2	4.0%	26955
ethylene	3171.5	8.0%	39644
propene	1325.4	1.1%	120489
propane	1939.2	2.1%	92343
CO	2218.7	20%	11094
H2	2137.6	80%	2672
Acetylene	1943	5%	38860